ＳＣＷ放射光と光核科学

1）　ＭｅＶガンマ線による科学

背景：平成14年9月19日に出された「原子力二法人の統合に関する報告書」でも、「光量子・射光利用研究では、光の量子的利用であるレーザーと世界最高性能の放射光施設であるSPring-8の放射光を利用して、核科学、核工学の研究や原子力材料等に係る基盤技術の開発に重点化することが適当である。」

2）　**日本学術会議での「光科学」推進策**

3）　SPring-8ウイグラ光からの単色放射光でパリティ非保存遷移測定実験、ニュースバルでの光核反応実験。加速器ビームラインでの逆コンプトンガンマ線発生

発展の様式（三位一体）

破壊→保守→創造→。。。。。

ＳPring-8**も**10**年。そろそろ保守から創造へ**

光の量子的利用→ 逆コンプトンガンマ線ビーム

1. SPring-8蓄積リング（8 GeV),ニュースバル（1.5 GeV)と
   レーザー光の掛け合わせによる新技術

2. 超伝導ウイグラーの開発

3. アルコールレーザー、
   大出力ＦＥＬ光の開発

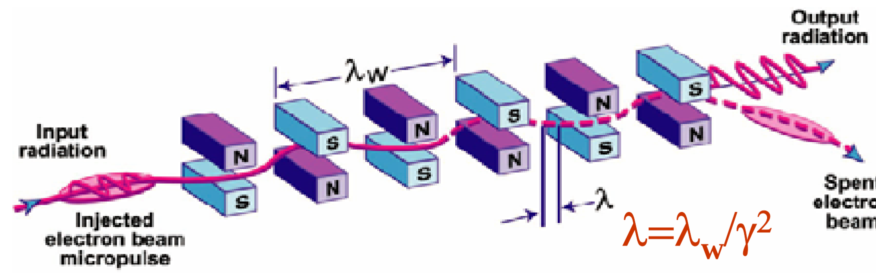

Fig. 1. Schematic illustration of the interaction between the electron beam and the wiggler in an FEL with a planar wiggler (2).

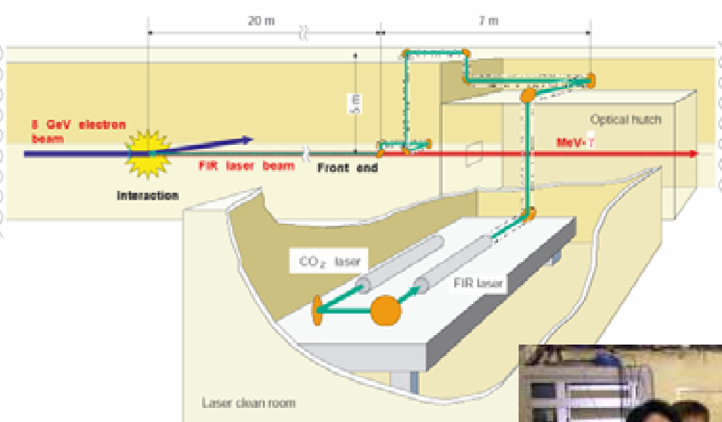

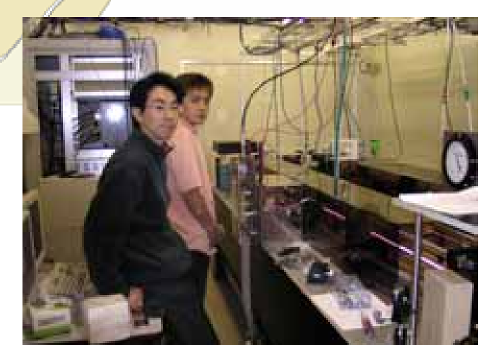

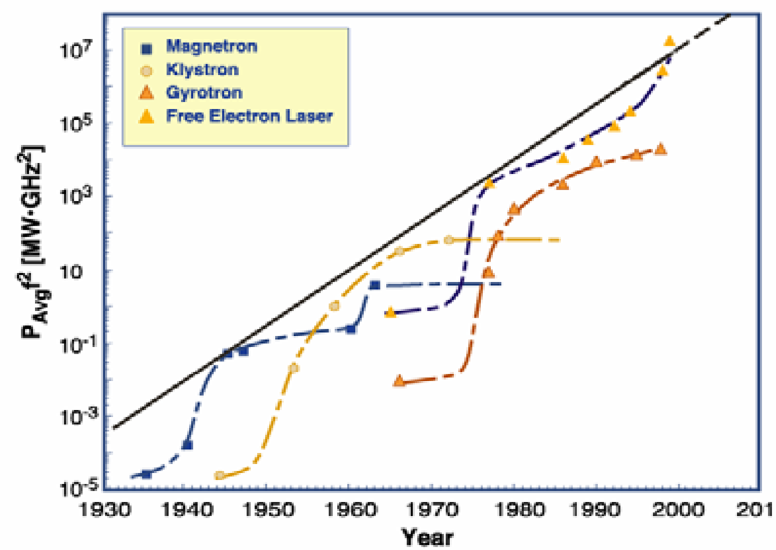

Fig. 2. Progress in the development of a variety of vacuum electronic sources of coherent radiation, as measured by the evolution of the product of the average power and the square of the frequency. [Adapted from (2)]

Science 292, 1853 (2001)

超伝導ウイグラーからの光

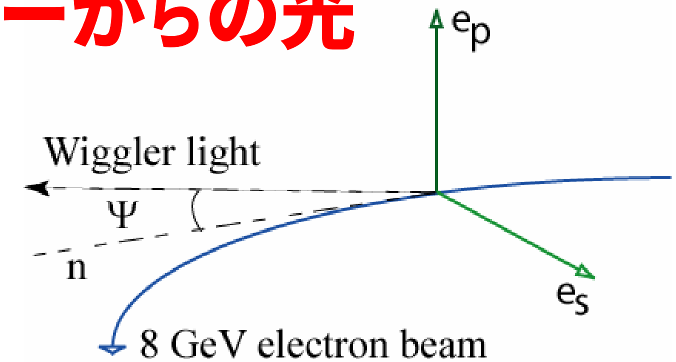

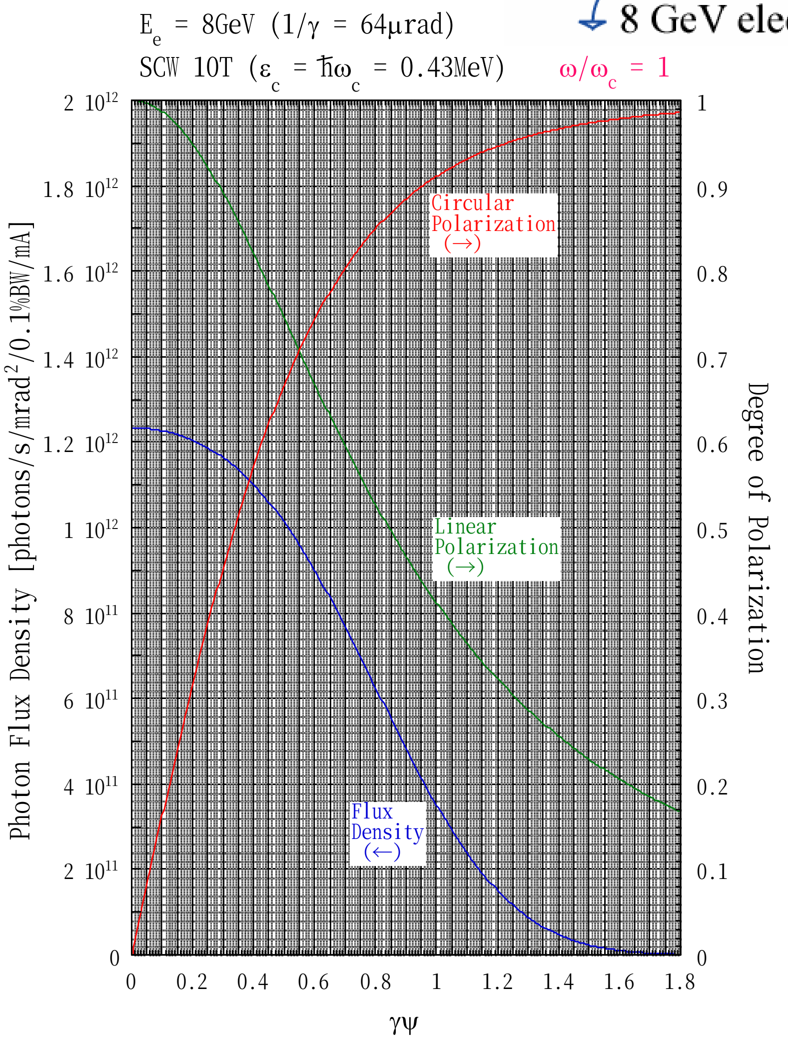

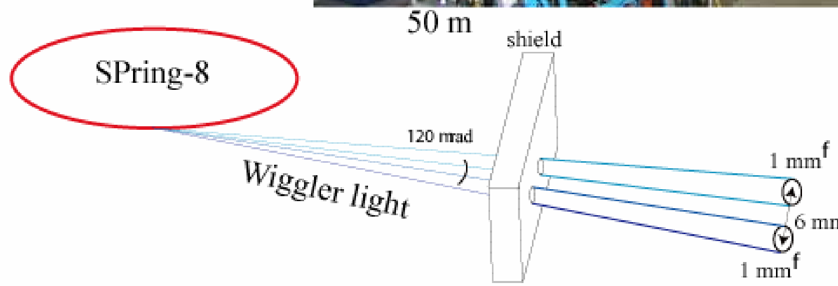

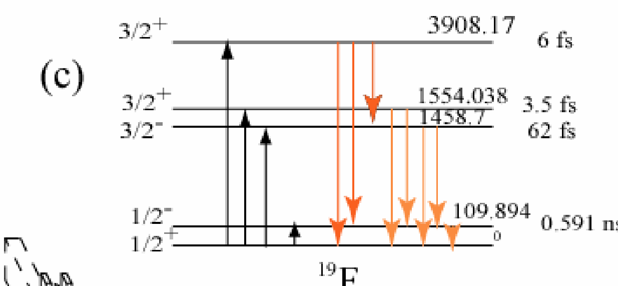

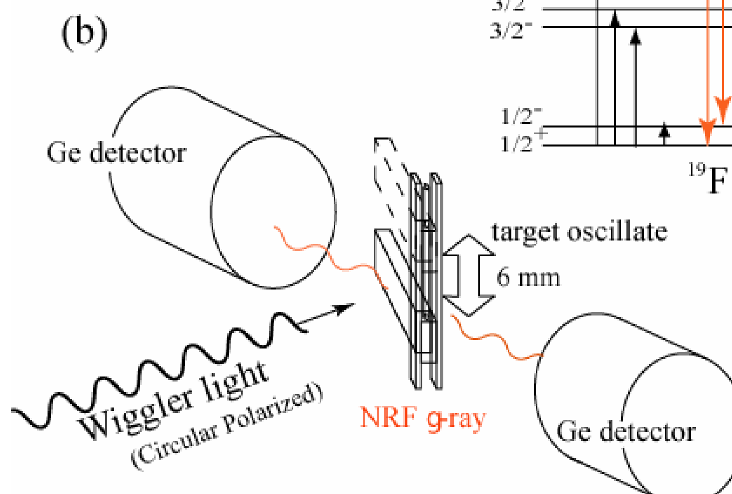

逆コンプトンガンマ線、ウイグラー光の利用

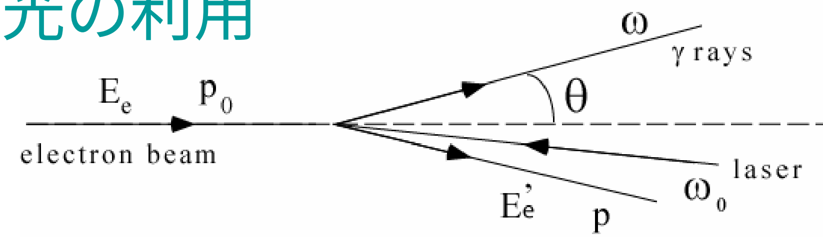

1. 宇宙での核反応を解明し、地球上での宇宙化石燃料であるウランに至るまでの、元素創生機構の解明、

2. 大強度、高偏極ガンマ線を用いた素粒子･原子核の構造の解明、

3. 偏極ガンマ線を用いた原子核励起、原子過程での基本的対称性の研究、

4. 10-30 MeV光量子ビームは放射性核変換への基礎研究に重要であり、この領域の光量子ビームはエネルギーと環境問題の解決に重要な役割を果たす、

5. 強力な光量子ビームからは光消滅による、偏極陽電子ビームが得られ、磁性研究などの新しいプローブとしても使われる可能性があり、ユニークな物質科学研究が展開される。

6. 新しい量子力学手法によるガンマ線、エックス線源の開発

光核反応による核物理、宇宙核物理、基本対称性

1. **パリティの破れの測定**

2. **光核反応による核構造研究**
   a) **核蛍光反応による低励起準位のＭ１，Ｅ１励起**
   b) **光核励起による集団運動、**
   c) **光核分裂、**

3. **原子核の**M1、E1**励起と宇宙核物理、**

光核反応による応用

1. **ガンマ線による核消滅研究**
   ^{129}I （$T_{1/2}$=1.6*10^7**年**）**など**

2. **光核反応中性子の工学的基礎研究、**

3. **磁気物性への期待**

4. **新しいガンマ線、エックス線源の期待**
   N^2効果

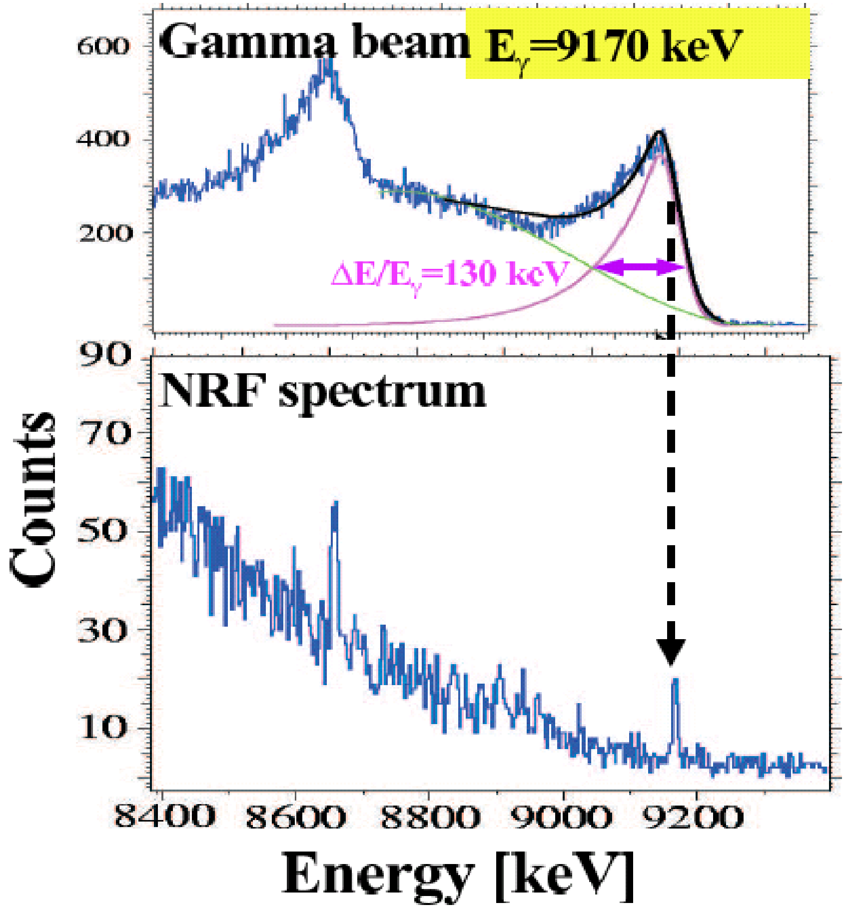

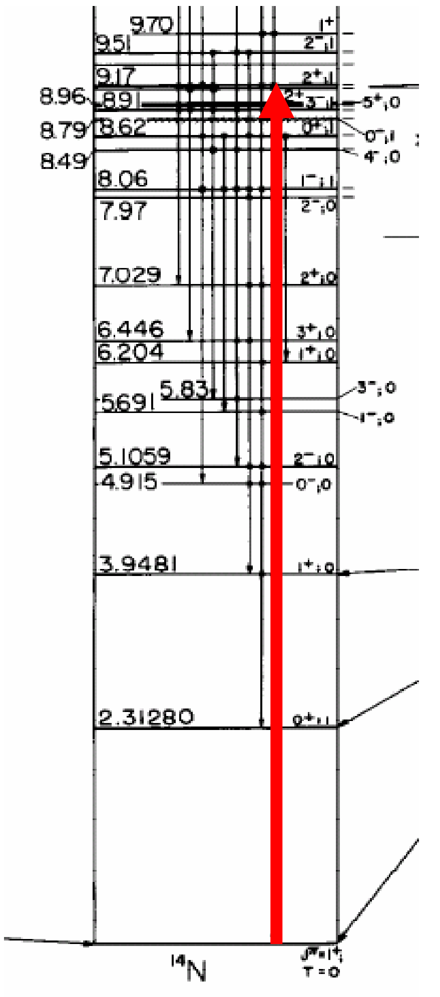

$$\sigma_{NRF} = 2\pi\left(\frac{\hbar c}{E_{NRF}}\right)^2 \frac{2J_f+1}{2J_i+1}$$

$$Y \propto 2\pi\left(\frac{\hbar c}{E_{NRF}}\right)^2 \frac{2J_f+1}{2J_i+1}\frac{\Gamma}{\Delta E_{beam}} \times N_t \times I_B$$

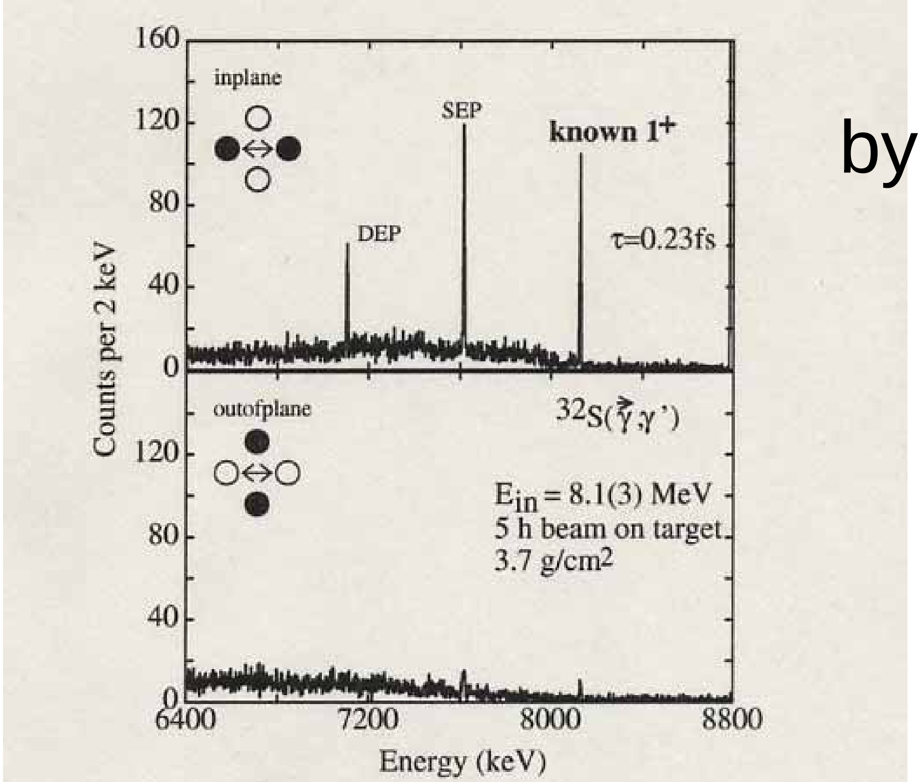

by Ohgaki et al.,

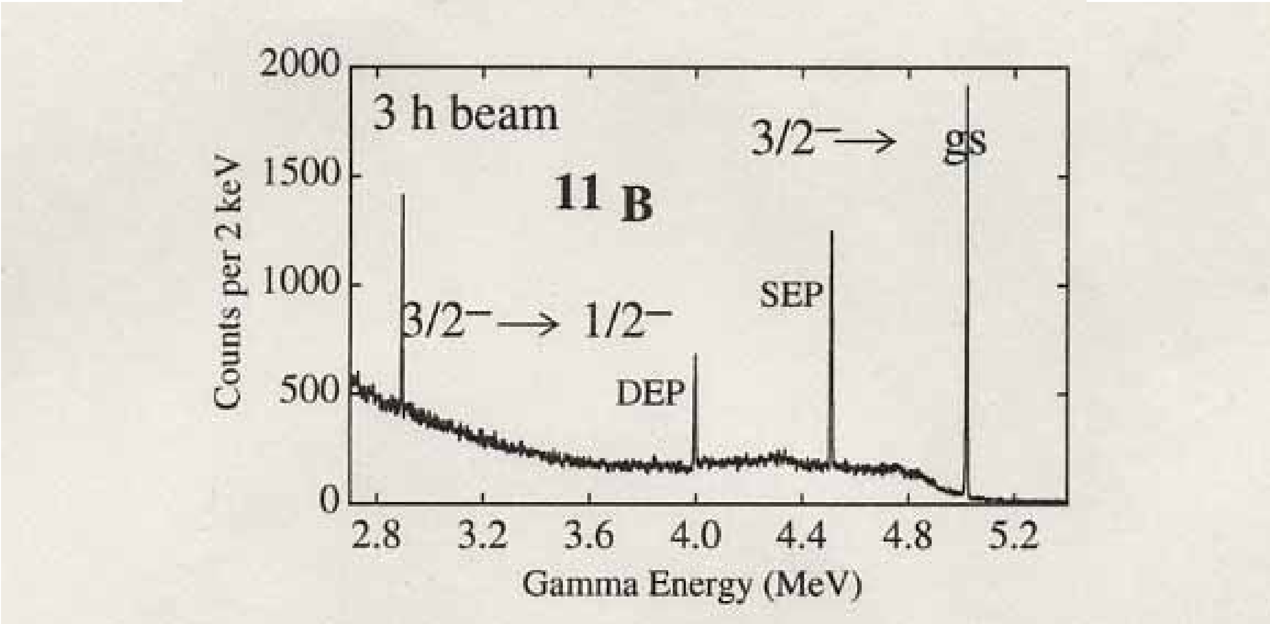

Excitation Modes in ^{11}B

^{11}B: Promising neutrino detection material
Prominent cluster structure

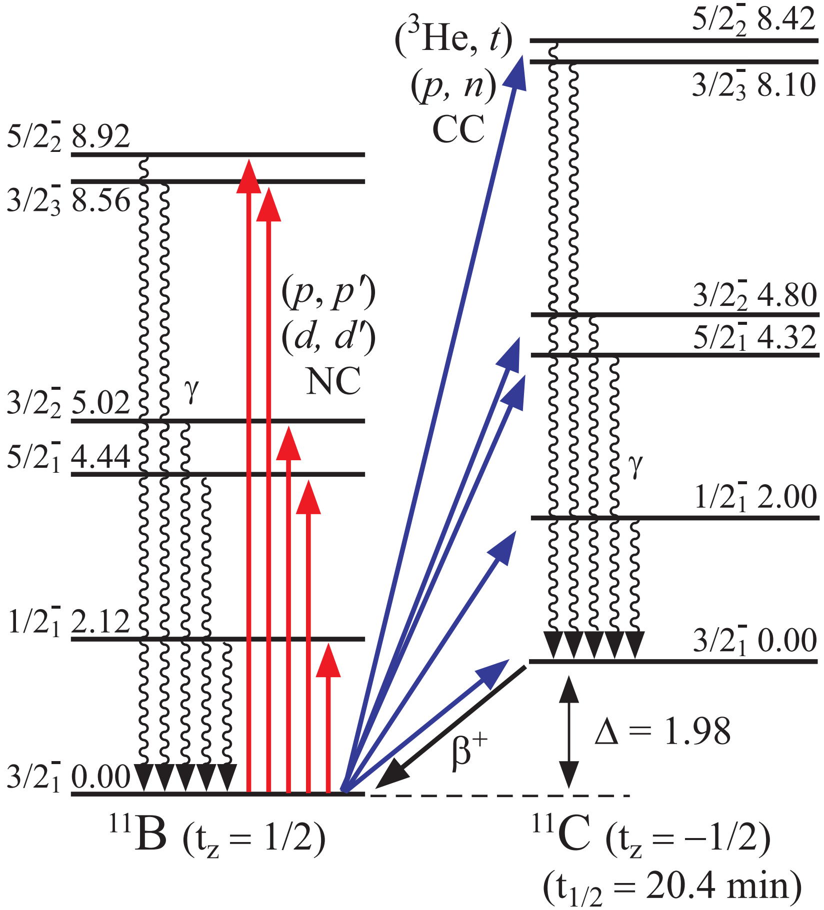

G.S. of ^{11}B is J^π=3/2$^-$ and T=1/2.

Excitation modes in ^{11}B are complex.

$$g.s.(3/2^-) \rightarrow 1/2^- \cdots (\Delta J^\pi = 1^+, 2^+) \otimes (\Delta T = 0, 1)$$
$$g.s.(3/2^-) \rightarrow 3/2^- \cdots (\Delta J^\pi = 0^+, 1^+, 2^+, 3^+) \otimes (\Delta T = 0, 1)$$
$$g.s.(3/2^-) \rightarrow 5/2^- \cdots (\Delta J^\pi = 1^+, 2^+, 3^+, 4^+) \otimes (\Delta T = 0, 1)$$

To extract the missing parts....

- Each ΔJ^π transition must be isolated.
- Isoscalar and isovector transitions must be separated.

Kawabata et al.

Kawabata et al.,

Measured Spectra

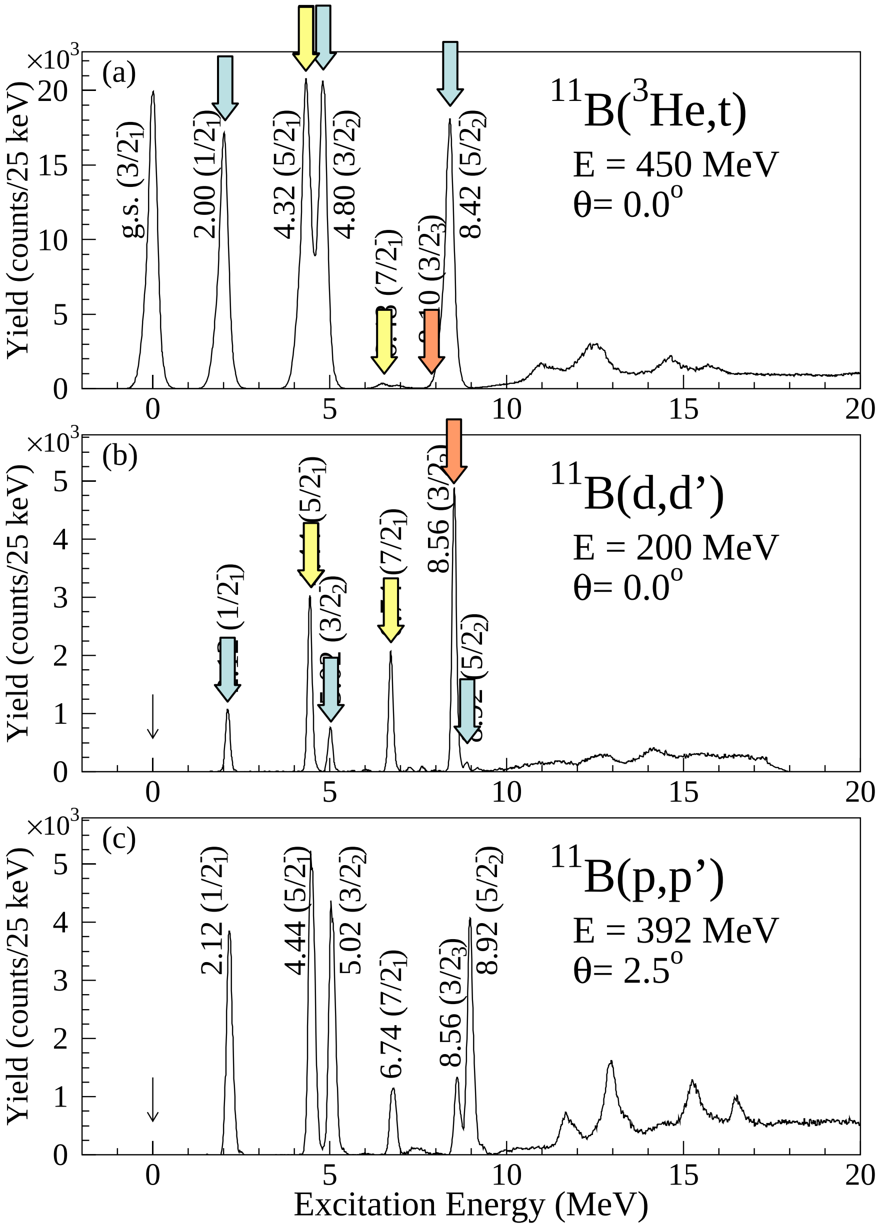

(^{3}He,t)

$V_{\sigma\tau}$ is strong.

Spin-flip transitions are dominant.

(d,d')

V_0 is strong.

Non-spin-flip transitions are dominant.

$1/2_1^-$, $5/2_1^-$, $3/2_2^-$, and $5/2_2^-$

M1 transitions are dominant.

$5/2_1^-$ and $7/2_1^-$

E2 transitions are dominant.

$3/2_3^-$

Unpredicted by SM calculation.

Non-spin-flip transition is dominant.

Expected to be a cluster state.

AMD (VAP) Calculation

Kawabata et al,

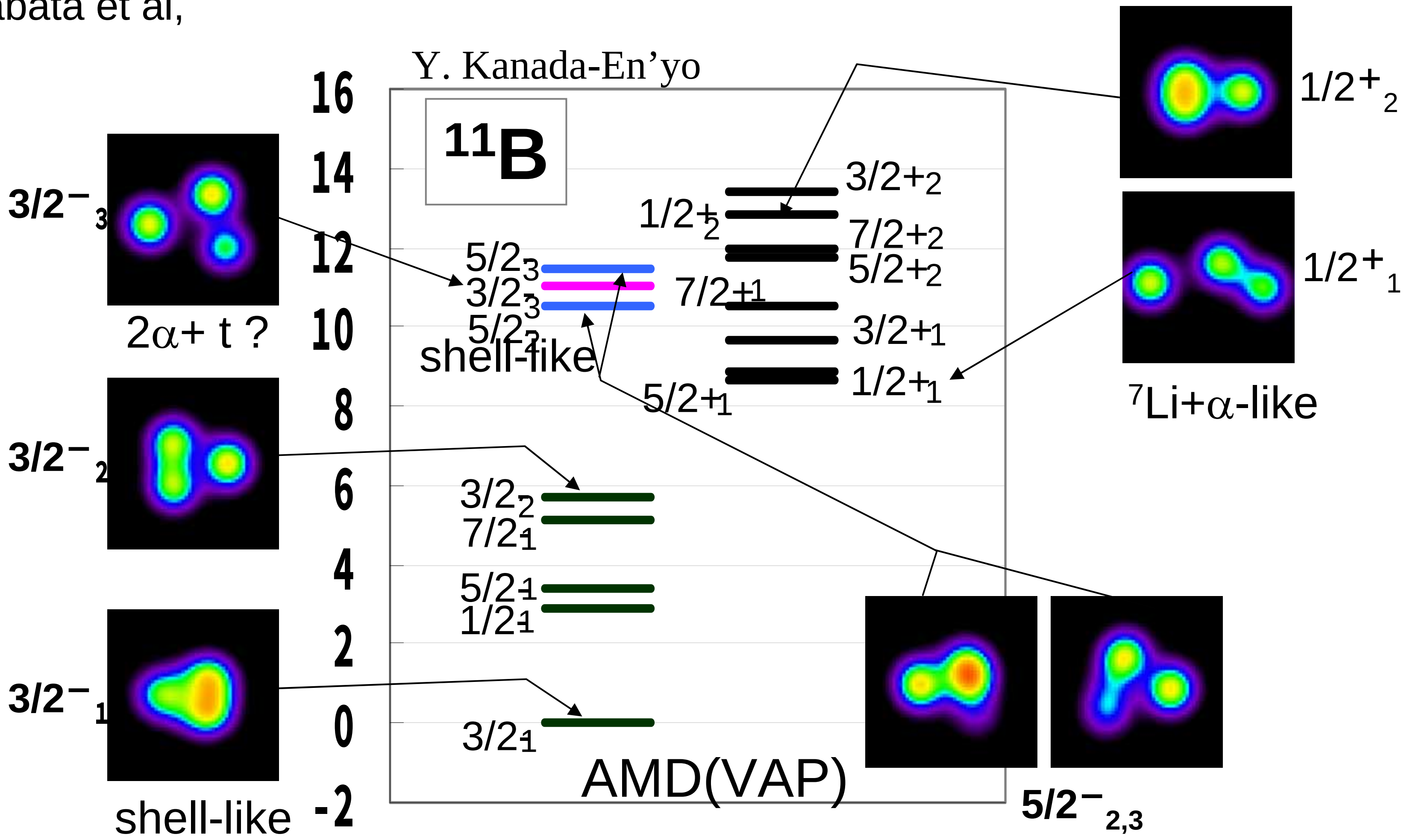

- AMD (VAP) calculation successfully predict the $3/2^{-}_{3}$ state with the 2α + t structure.
- The $5/2^{-}_{2}$ and $5/2^{-}_{3}$ states were described as a mixture of the SM and cluster components.
- Lower states have shell-like structures.

Kawabata et al.,

Analogous Relation

Analogous relation between $3/2^-_3$ state in ^{11}B and 0^+_2 state in ^{12}C is speculated

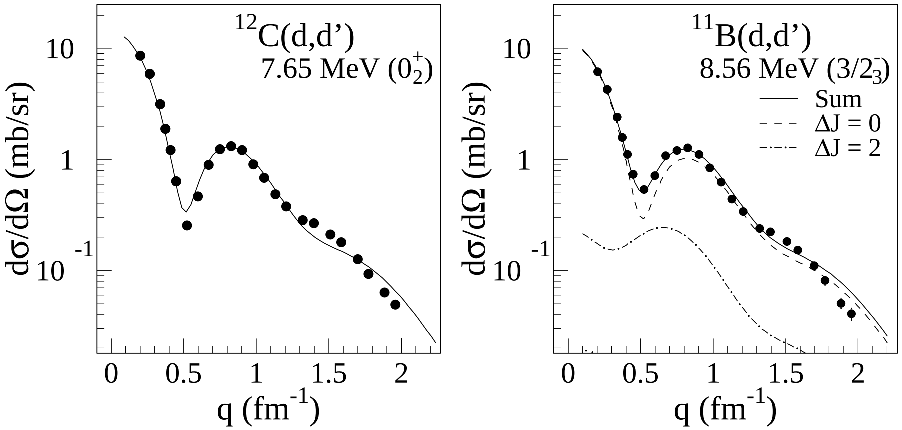

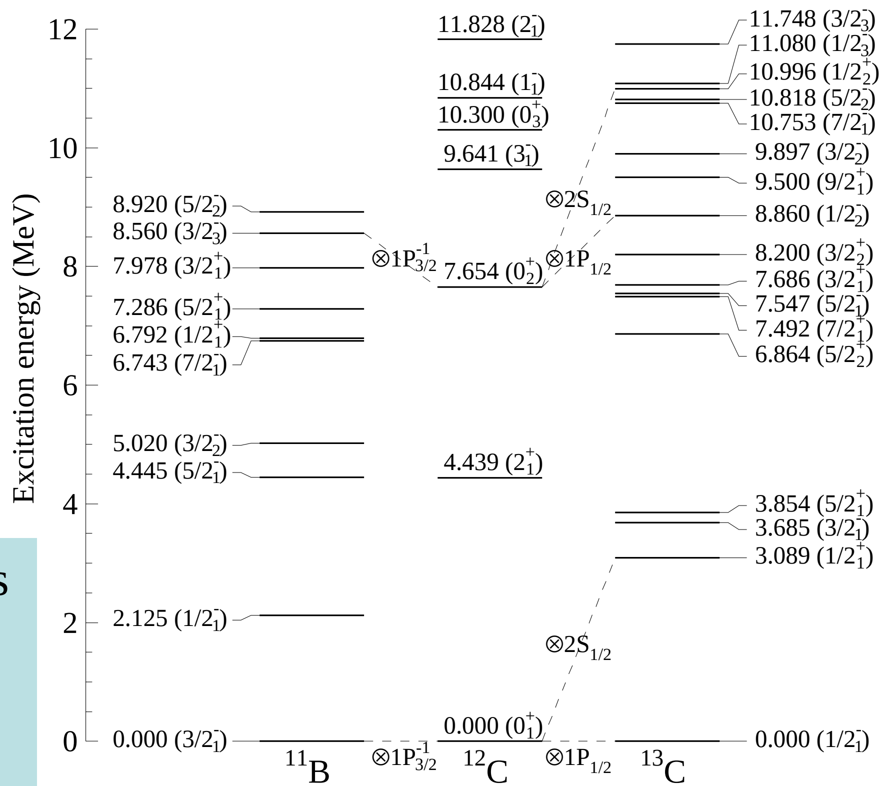

- Strong $\Delta J^\pi = 0^+$ component implies an analogous relation with 0^+_2 in ^{12}C.
  - 0^+_2 in ^{12}C has a 3α dilute cluster structure.
  - Possibly $3/2^-_3$ in ^{11}B has a dilute 2α+t structure.
- Similar analog relations are also expected in ^{13}C.

^{11}B, ^{13}C(α,α’) experiment will be performed in October.

大久保茂男さんの最近の話から

^{40}Ca での α+^{36}Ar クラスター状態 K=0^{-}バンドの予言と発見

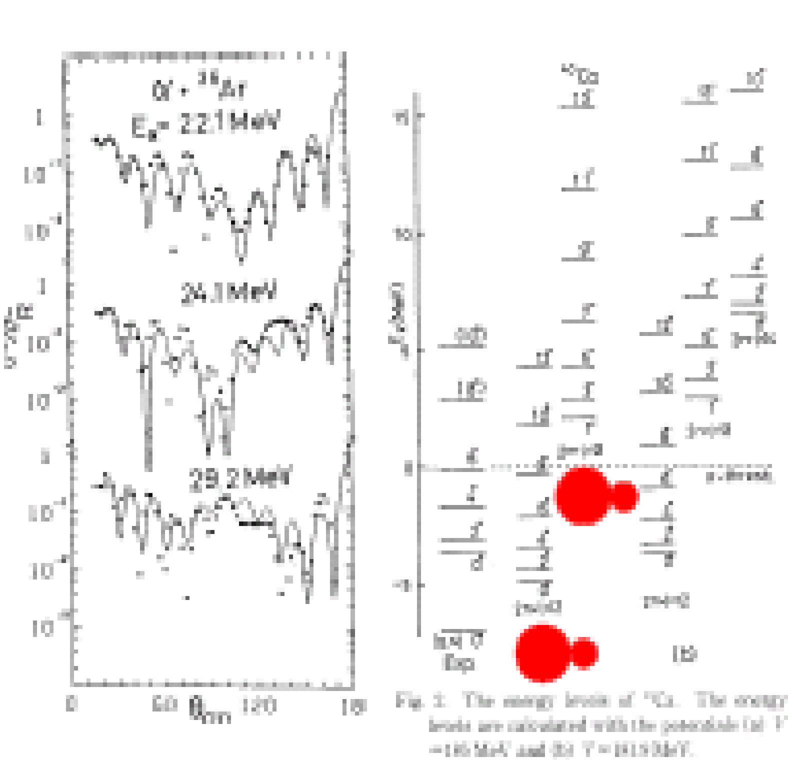

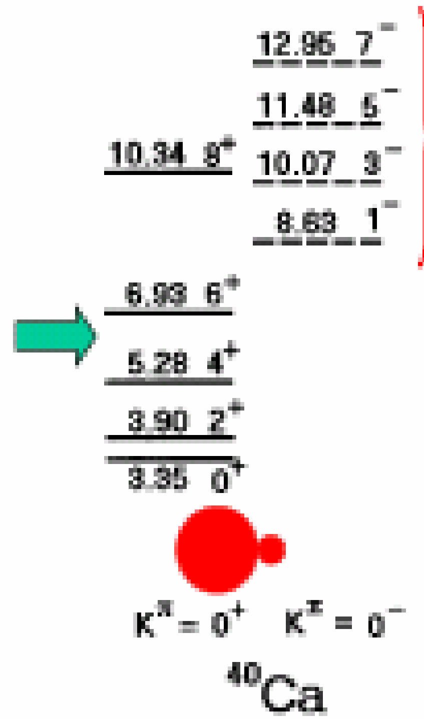

理論的予言

RCNPでの山屋らの実験結果(1993 PLB)

Yamagata, Akimune, Utsunomiya, et al.,

Excitation of Dipole Resonance in ^{4}He in the α cluster of ^{6,7}Li

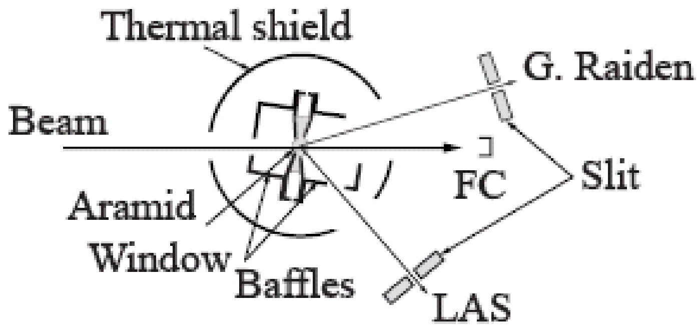

FIG. 1: A schematic view of the experimental setup.

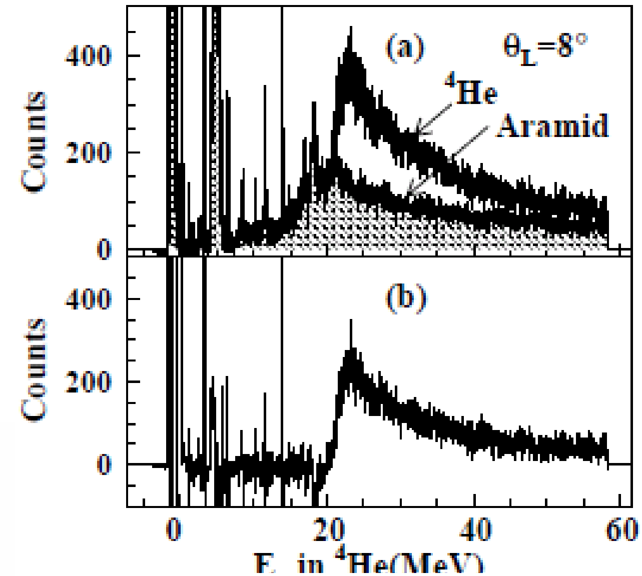

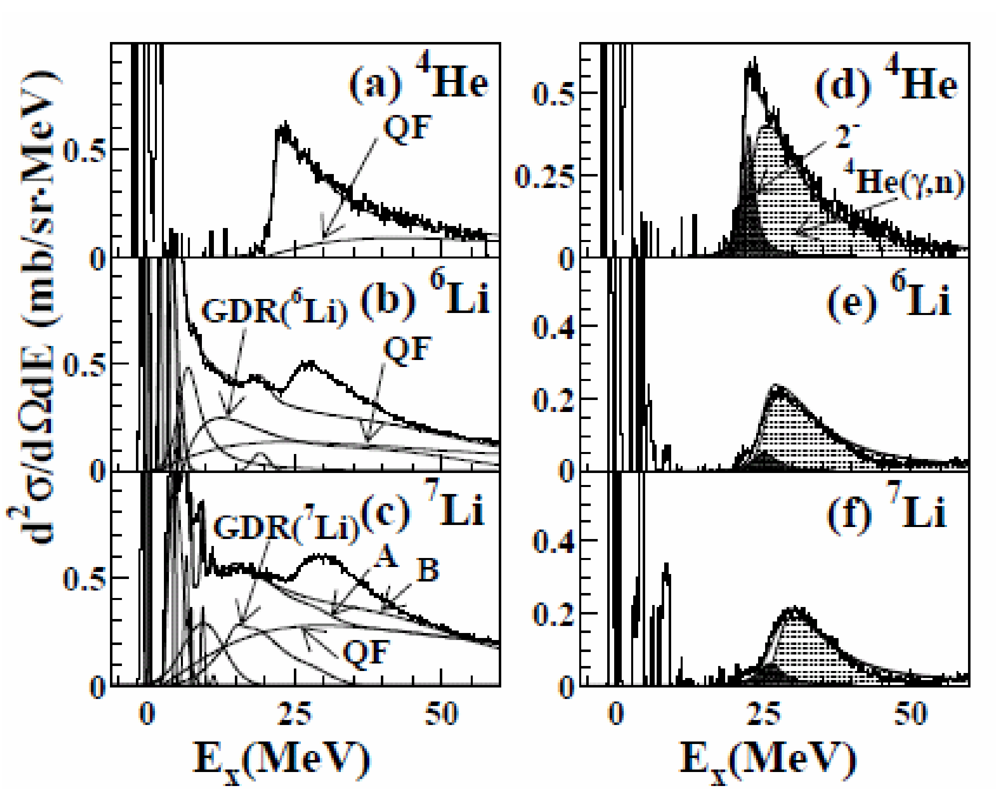

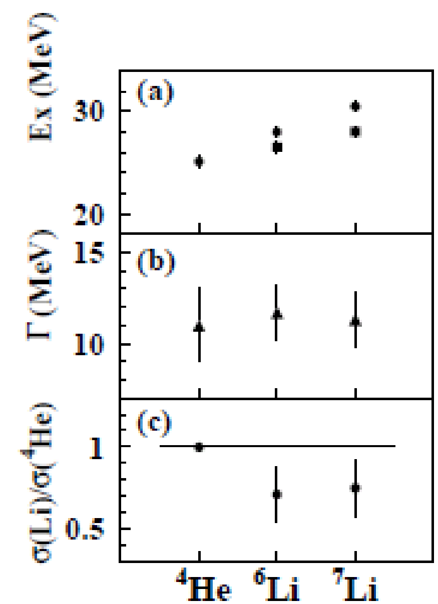

Parity Non Conservation Measurements with Photons at Spring-8

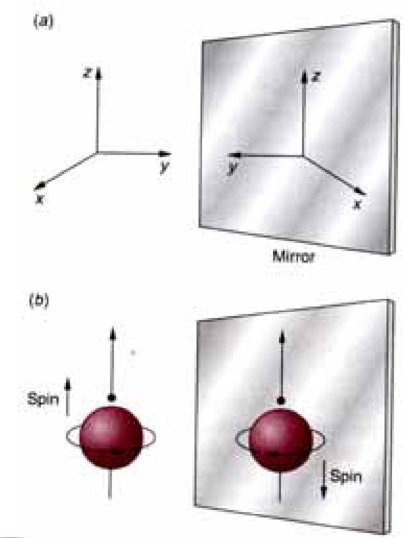

1. β-decay: T.D.Lee and C.N. Yang, Phys. Rev. 104 (1956).
2. Exp.: C.S. Wu et al., Phys. Rev. 105 (1957) 1413.
3. γ-decay: ^{181}Ta N. Tanner, Phys. Rev. 107, 1203 (1957).
4. -6×10^{-6}: V.M. Lobashov et al., JETP Lett. 5, 59 (1967); Phys. Lett. 25B 104 (1967).
5. Anapole moment: Ya. B. Zeldovich, Sov. Phys. JETP 6, 1184 (1958).
6. C.S. Wood et al., Science 275, 1759 (1997).

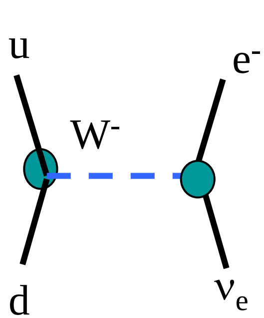

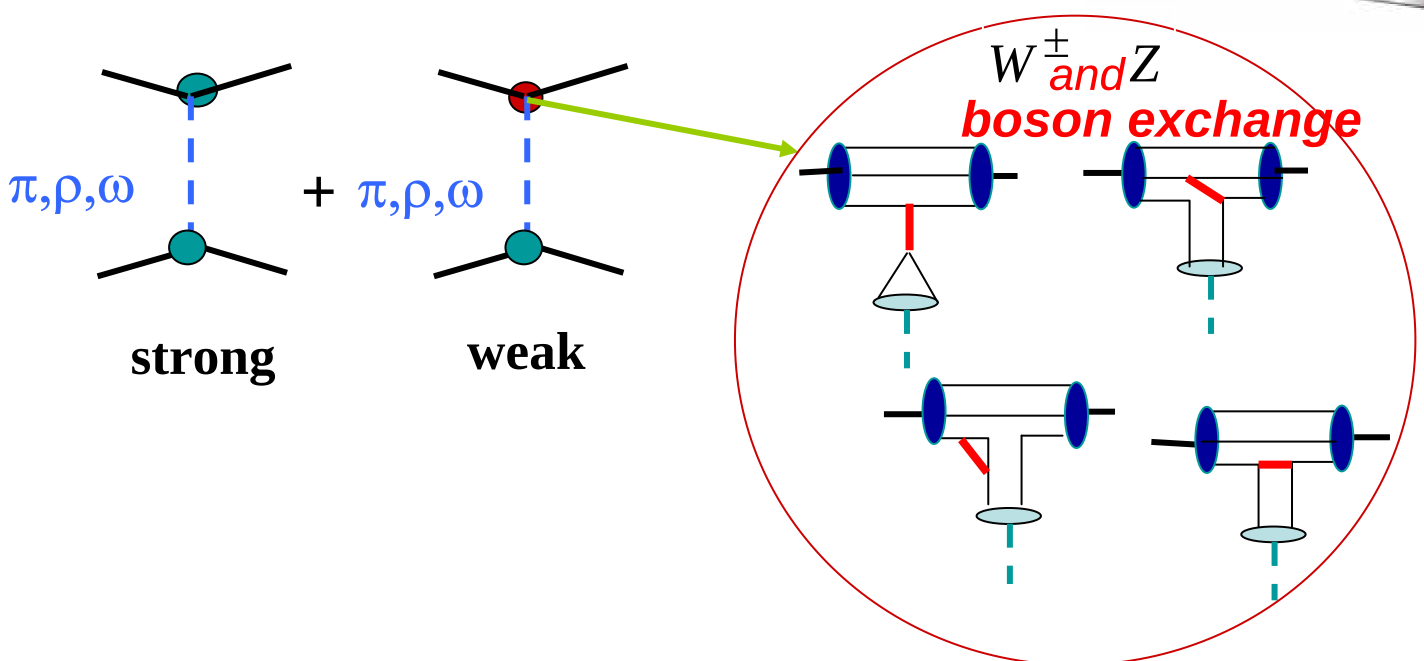

Two states perturbation

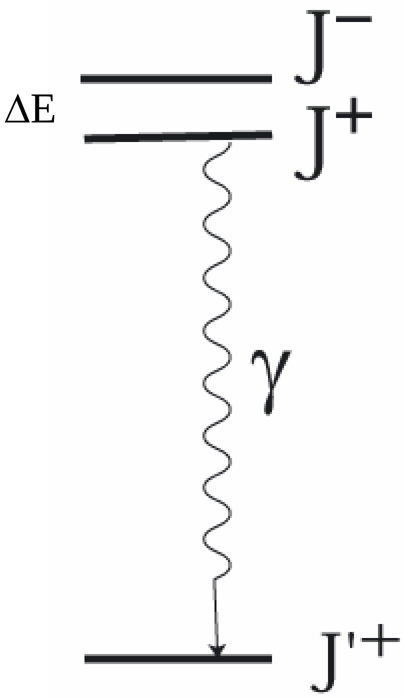

$$|\psi_{J^+}\rangle = \cos(\varepsilon)|\phi_{J^+}\rangle + \sin(\varepsilon)|\phi_{J^-}\rangle$$

$$|\psi_{J^-}\rangle = \cos(\varepsilon)|\phi_{J^-}\rangle - \sin(\varepsilon)|\phi_{J^+}\rangle$$

$$\sin(\varepsilon) \doteq \varepsilon = \frac{\langle\phi_{J^-}|H_{pnc}|\phi_{J^+}\rangle}{E_+ - E_-} = 10^{-6} - 10^{-2}$$

$$\cos(\varepsilon) \doteq 1$$

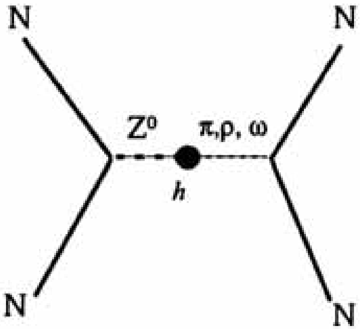

$$H_{PNC} = \sum_{i=1}^{A} \frac{g_S + g_V\tau_3(i)}{2M}\, \vec{\sigma}(i)\cdot\vec{p}(i)$$

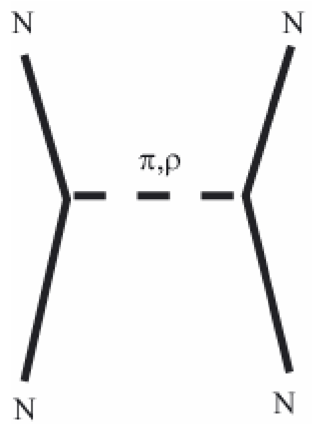

Nuclear force by meson exchange

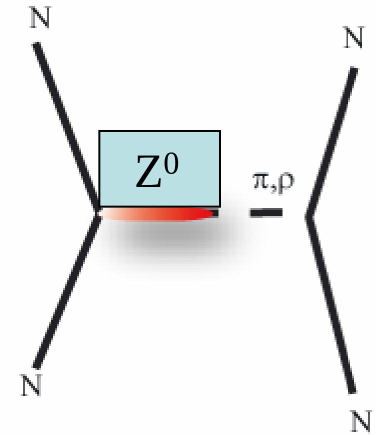

Parity violation interaction for NN

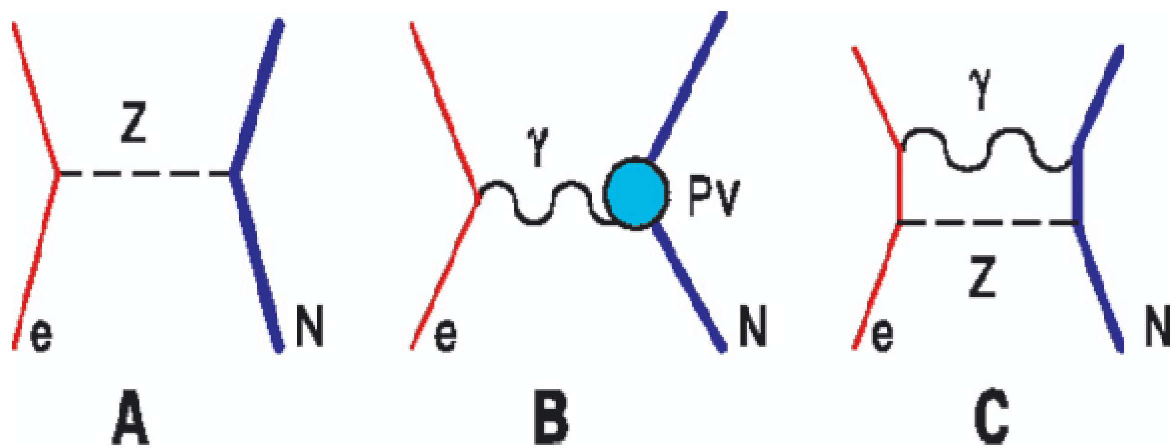

Parity violation force via electromagnetic interactions

Desplanques, Donoghue and Holstein (DDH) [1] as

$$
\begin{aligned}
V^{PNC}(i,j) &= i\frac{f_\pi g_{\pi NN}}{\sqrt{2}}\left(\frac{\tau_i\times\tau_j}{2}\right)_z(\sigma_i+\sigma_j)\cdot\mathbf{u}_\pi(\mathbf{r}) \\
&-g_\rho\left(h_\rho^0\tau_i\cdot\tau_j+h_\rho^1\left(\frac{\tau_i+\tau_j}{2}\right)_z+h_\rho^2\frac{(3\tau_i^z\tau_j^z-\tau_i\cdot\tau_j)}{2\sqrt{6}}\right) \\
&\times((\sigma_i-\sigma_j)\cdot\mathbf{v}_\rho(\mathbf{r})+i(1+\chi_V)(\tau_i\times\tau_j)\mathbf{u}_\rho(\mathbf{r}))-g_\omega\left(h_\omega^0+h_\omega^1+\left(\frac{\tau_i+\tau_j}{2}\right)_z\right) \\
&\times((\sigma_i-\sigma_j)\cdot\mathbf{v}_\omega(\mathbf{r})+i(1+\chi_S)(\tau_i\times\tau_j)\mathbf{u}_\omega(\mathbf{r}))-(g_\omega h_\omega^1-g_\rho h_\rho^1)+\left(\frac{\tau_i-\tau_j}{2}\right)_z \\
&\times(\sigma_i+\sigma_j)\cdot\mathbf{v}_\omega(\mathbf{r})-g_\rho h_\rho'^1 i\left(\frac{\tau_i\times\tau_j}{2}\right)_z(\sigma_i+\sigma_j)\cdot\mathbf{u}_\omega(\mathbf{r}).
\end{aligned}
$$

Weak coupling

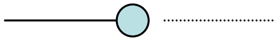

$f_\pi,\ h_\rho^0,\ h_\rho^1,\ h_\rho^2,\ h_\omega^0,\ h_\omega^1$

M. Fujiwara and A.I. Titov, PRC 68, 065503 (2004)

Expected asymmetry -5×10^{-8}

2.2 MeV

γ ray emission

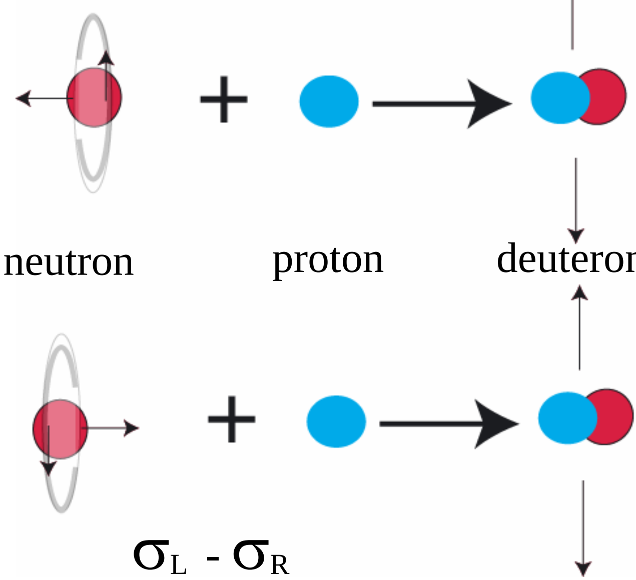

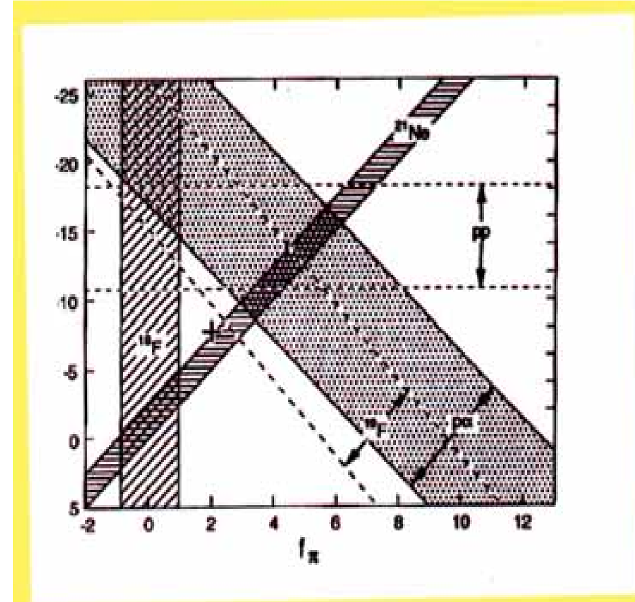

$$A\gamma = \frac{\sigma_L - \sigma_R}{\sigma_L + \sigma_R}$$

LANL project

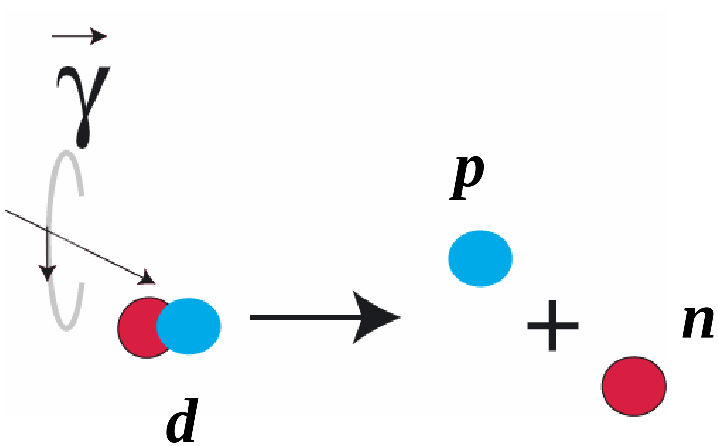

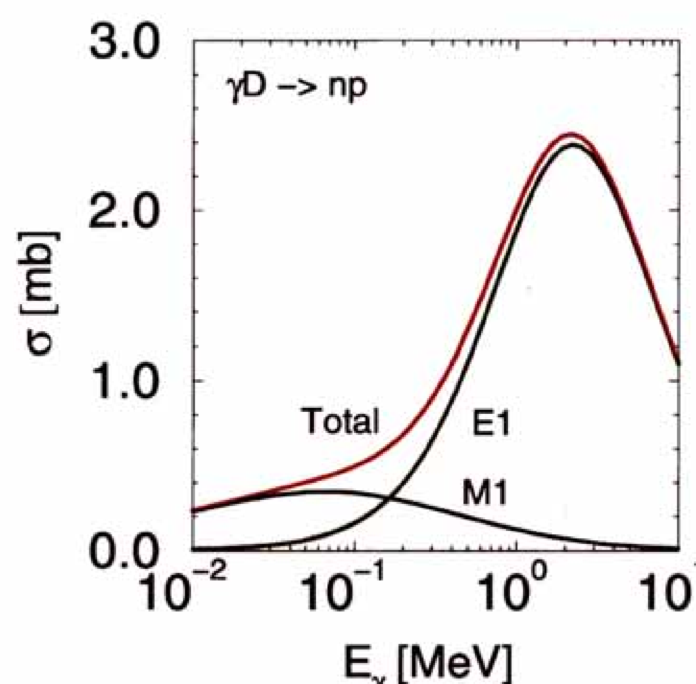

M. Fujiwara and A.I. Titov, Phys. Rev. C 68, 065503 (2004)

PNC transitions in np-system

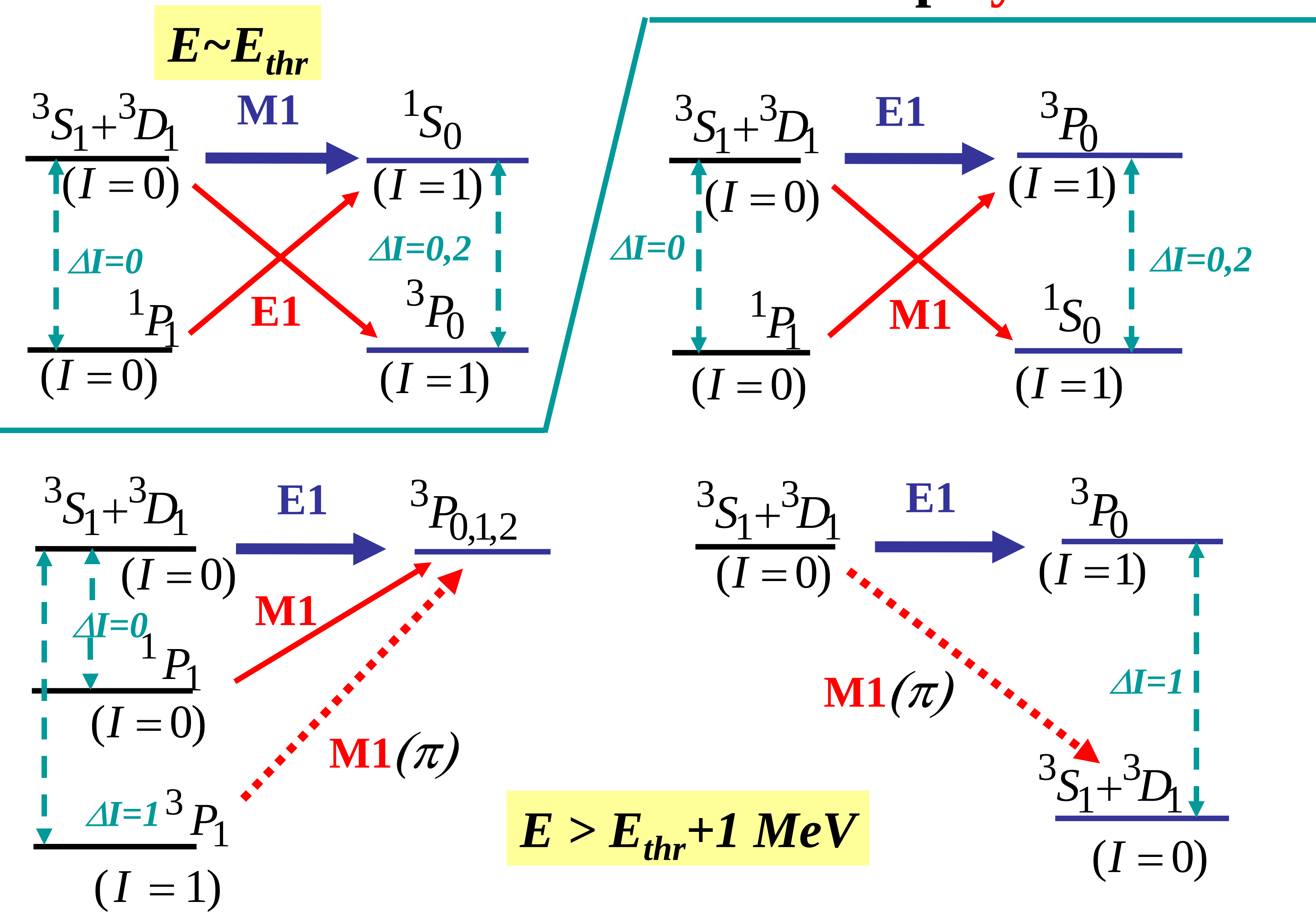

Total cross section of deuteron photo-disintegration

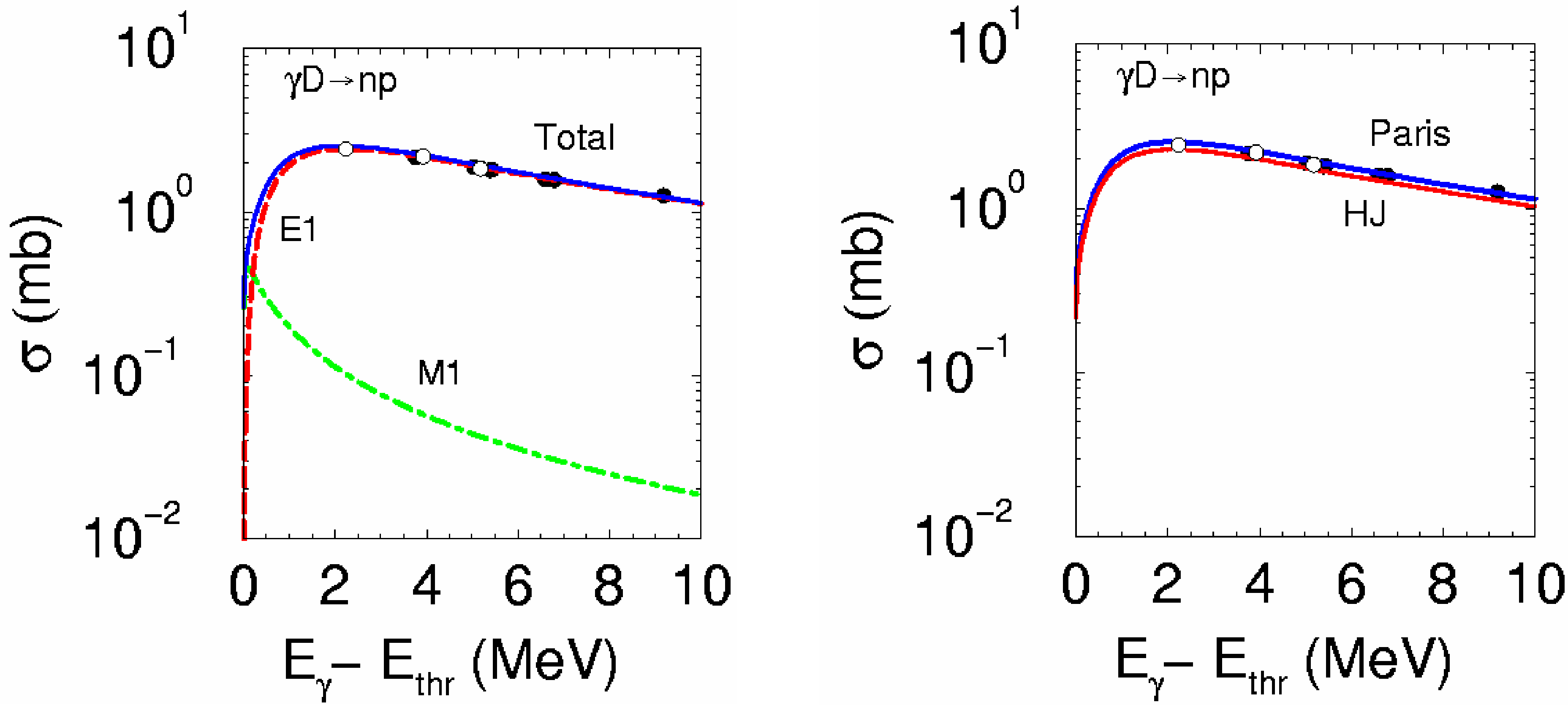

M. Fujiwara and A.I. Titov, PRC 69, 065503 (2004)

High sensitivities for short range interactions

PNC asymmetry:polarized beam and unpolarized target

$$A_{RL}^{PNC}(E_\gamma) = 2\frac{M1 \otimes \Delta E1_V + E1 \otimes \Delta M1_V + E1 \otimes \Delta M1_\pi}{M1^2 + E1^2}$$

$$|\Delta M1(\pi)| = |\pi_1 + \pi_2| << |\pi_{1.2}|$$

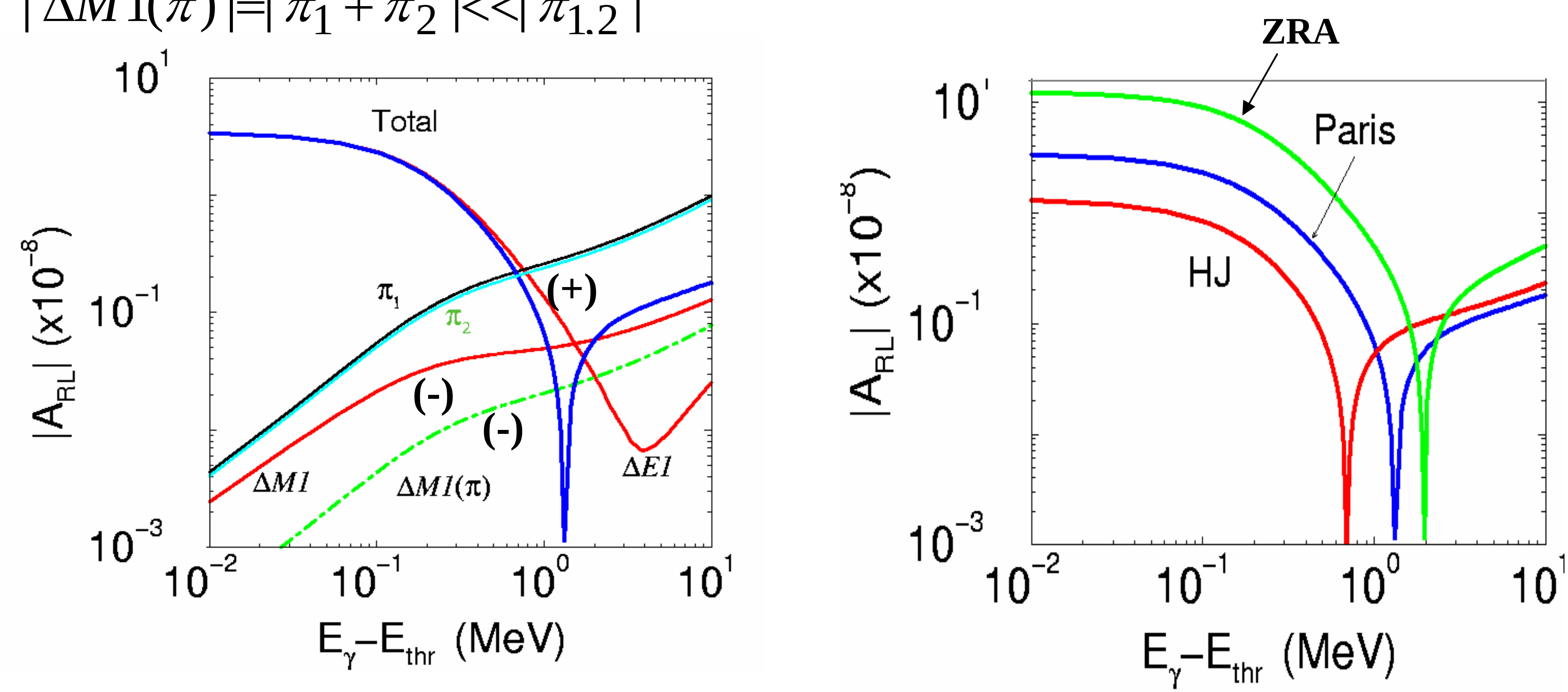

One experiment on deuteron give a strong constrant.

we found a principle possibility
to find constraints for PNC coupling constants
using only the simplest nuclear object: np-system

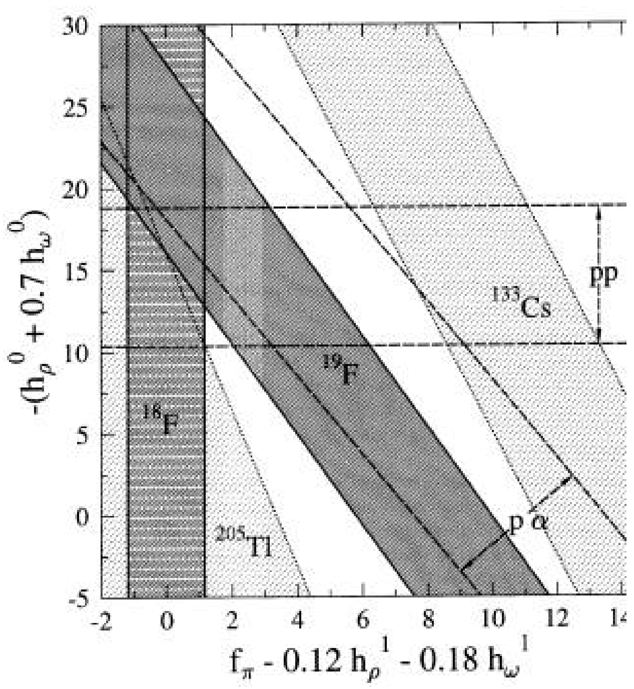

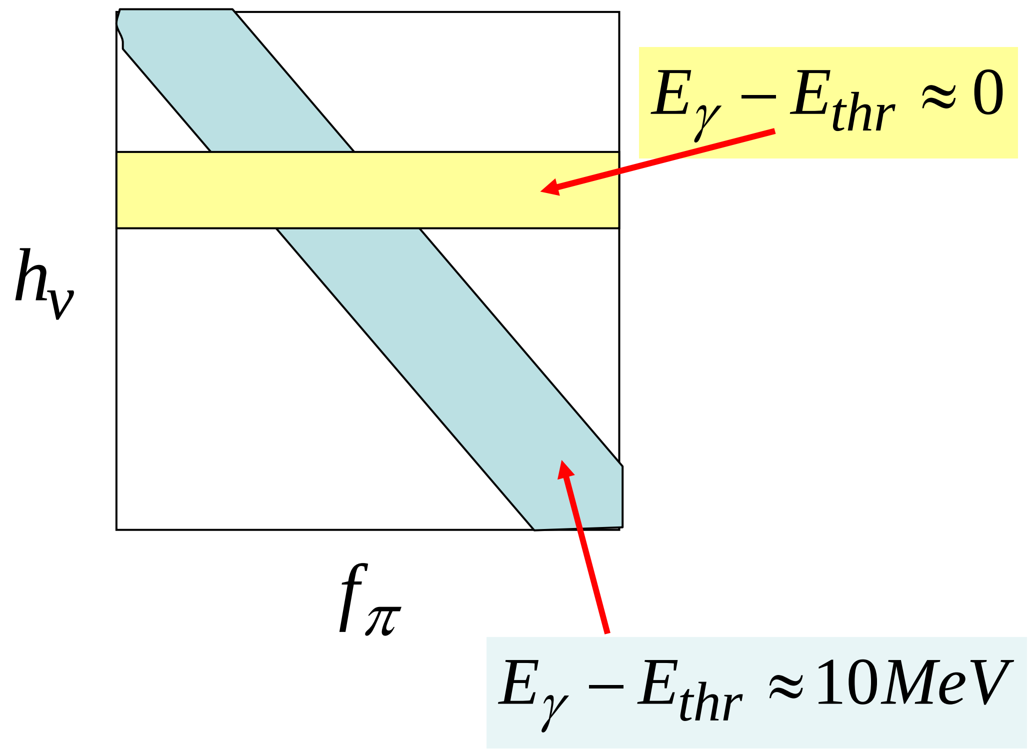

M. Fujiwara and A.I. Titov, Phys. Rev. C 69, 065503 (2004).

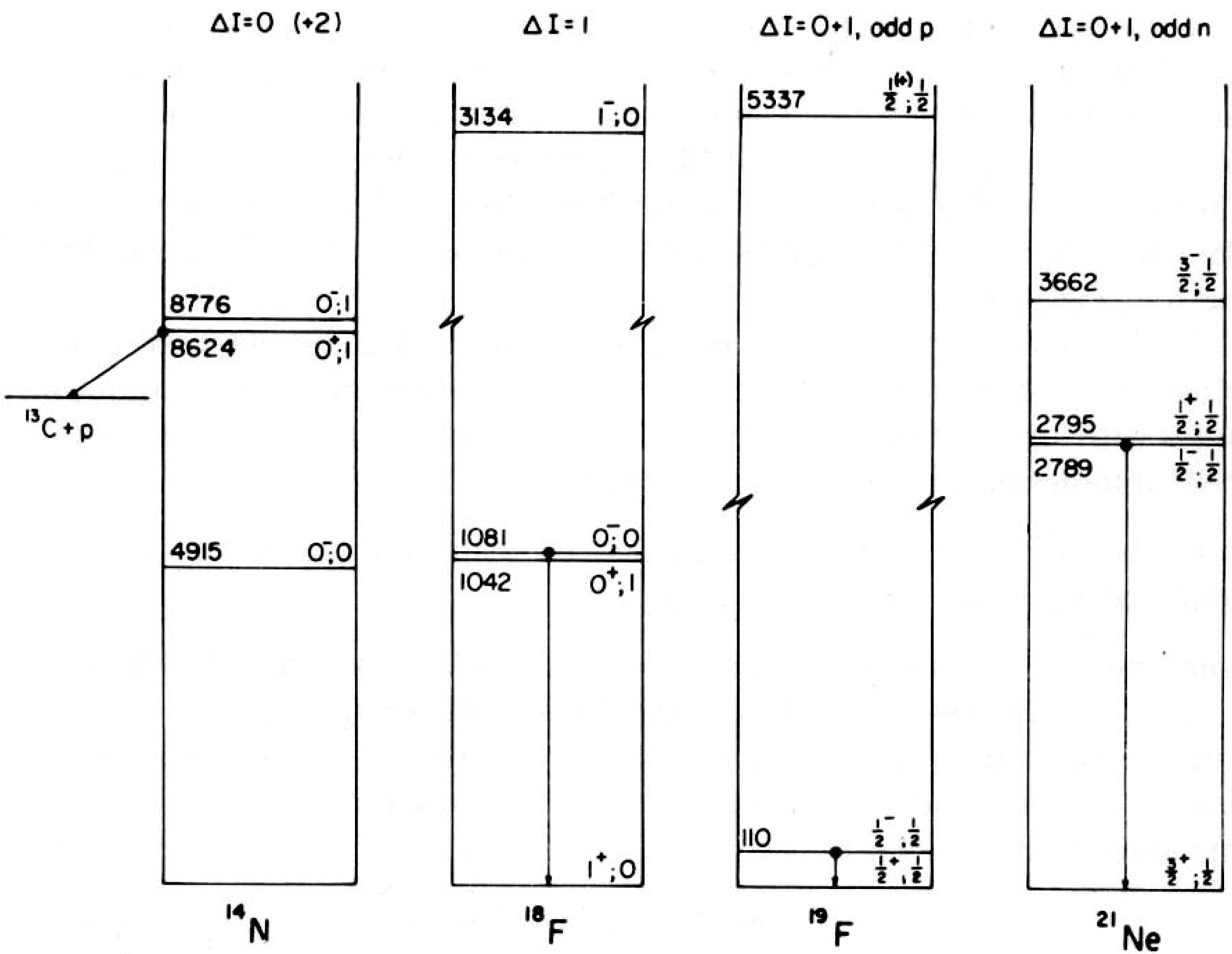

ΔE	152−206i keV	39 keV	110 keV	5.7 keV
ΔE′	3703 keV	3134 keV	5337 keV	3662 keV
	$\sqrt{\Gamma_{0^-}/\Gamma_{0^+}} = 10.5$	$\lvert M1/E1 \rvert = 112$	$M1/E1 = 11$	$\lvert M1/E1 \rvert = 296$

M1 and E1 excitations and PNC experiments

K.S. Krane et al., PRL 26, 1579 (1971).
PRC 4, 1906 (1971).
B. Jenschke and P. Bock, PL 31B, 65 (1970).
E.D. Lipson, F. Boehm and J.C. van den Leeden, PL 35B, 307 (1971)
W.V. Yuan et al., Phy. Rev. C44, 2187 (1991).

Parity violation in neutron absorption

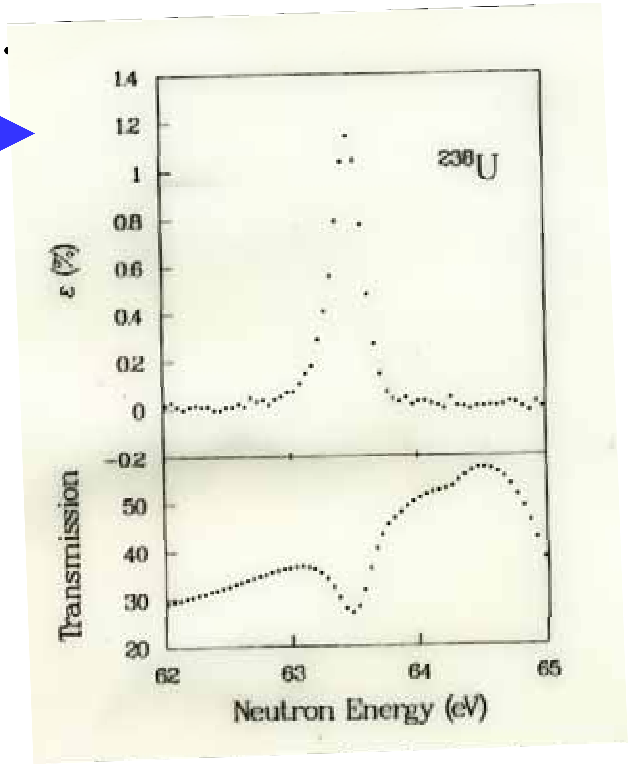

In NRF …

The doorway state for parity violation interaction is dipole resonances (isovector and isoscalar).

Therefore, statistical treatment is essential to analyze the PNC effect.

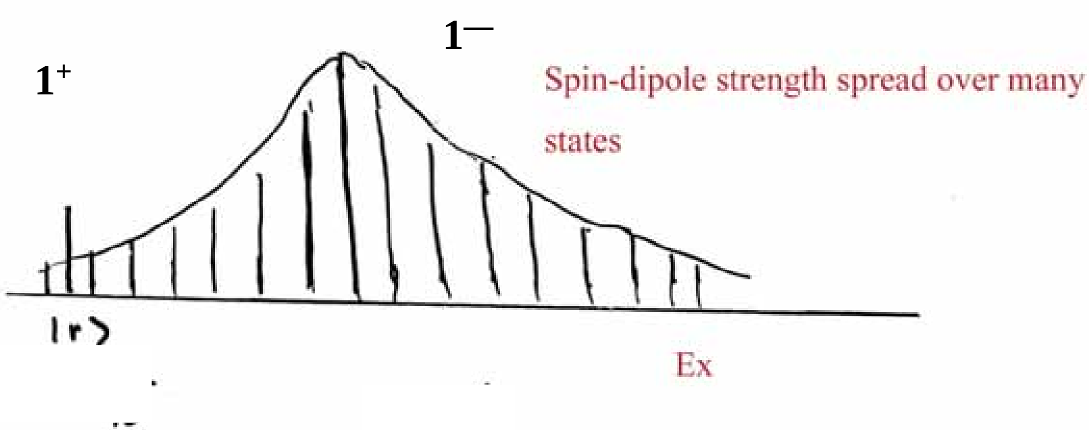

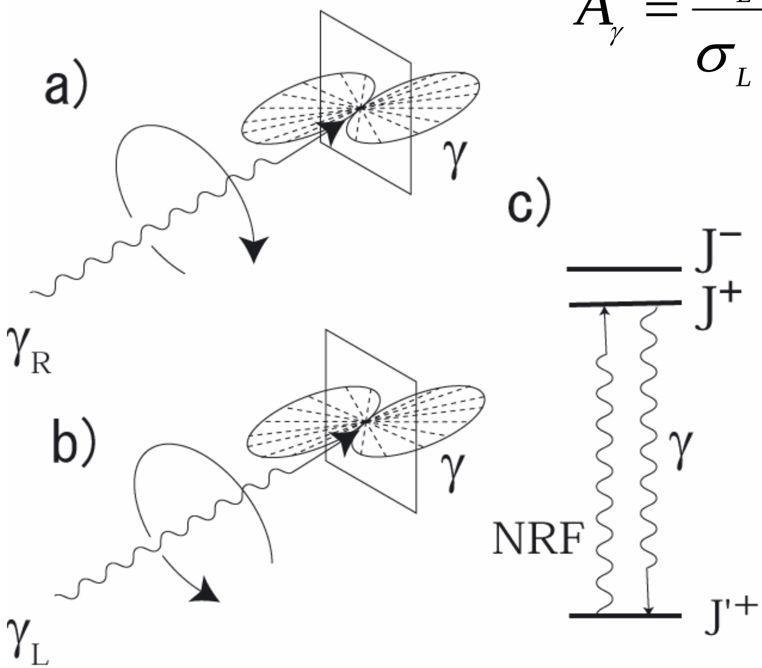

$$A_\gamma = \frac{\sigma_L - \sigma_R}{\sigma_L + \sigma_R} = 2\varepsilon T(M1)/T(E1) \quad or \quad 2\varepsilon T(E1)/T(M1)$$

E1 excitation

M1 excitation

1. Direct counting of NRF yields
2. Both E1 and M1 excitations are used.
3. Self-corrections for experimental error
4. Circular polarized beam with high stability and High emittance is needed.

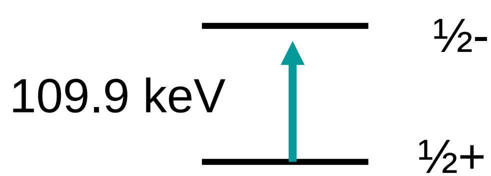

In the case of ^{19}F

1 eV

$$A\gamma = 2\,\frac{\langle \phi_{J^-} | H_{pnc} | \phi_{J^+} \rangle}{E_+ - E_-}\;\frac{T(E1)}{T(M1)}$$

10 – 100 keV

10 - 300

$$A_\gamma = \frac{2}{\Delta E}\left\langle \frac{1}{2}^+ \middle| H_{PNC} \middle| \frac{1}{2}^- \right\rangle \left(\frac{\langle 1/2^+|\mu|1/2^+\rangle - \langle 1/2^-|\mu|1/2^-\rangle}{\langle 1/2^+|O(E1)|1/2^-\rangle} \right)(1+\cos\theta)$$

NRF cross section at resonance energy E_{NRF}

$$\sigma_{NRF} = \frac{\pi}{2}\left(\frac{\hbar c}{E_{NRF}}\right)^2 \frac{2J_f+1}{2J_i+1}\frac{\Gamma^2}{(E-E_r)^2+\frac{1}{4}\Gamma^2}$$

E_{NRF} (MeV)	σ_{NRF} (10^{-24} cm^2)
0.1	$2\text{x}10^5$
1.0	$2\text{x}10^4$
10.0	$2\text{x}10^3$

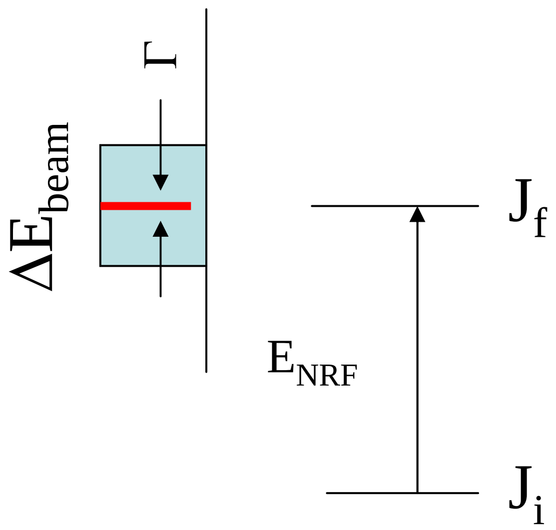

$$Y \propto 2\pi\left(\frac{\hbar c}{E_{NRF}}\right)^2 \frac{2J_f+1}{2J_i+1}\frac{\Gamma}{\Delta E_{beam}} \times N_t \times I_B \times P_D(T, E-E_{NRF})$$

We can use very thin targets if the resolution is excellent !!

A.I. Titov, M. Fujiwara and K. Kawase et al.,

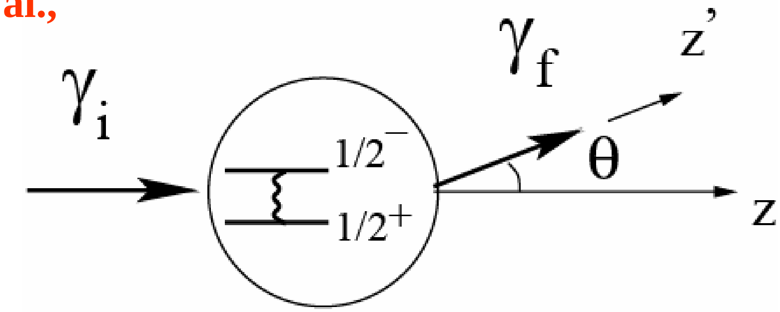

^{19}F

$$1/2^+ \rightarrow 1/2^- \rightarrow 1/2^+$$

$$A_{RL} = \frac{2}{\Delta E}\left\langle \frac{1}{2}^+ \middle| H_{PNC} \middle| \frac{1}{2}^- \right\rangle \left(\frac{\langle 1/2^+ | \mu | 1/2^+ \rangle - \langle 1/2^- | \mu | 1/2^- \rangle}{\langle 1/2^+ | O(E1) | 1/2^- \rangle} \right) (1 + \cos\theta)$$

$$1^+ \rightarrow 0^- \rightarrow 1^+ \qquad {}^{18}\mathrm{F}$$

$$A_{RL} = \frac{2}{\Delta E}\langle 0^- | H_{PNC} | 1^+ \rangle \left(\frac{\langle 0^+ | O(M1) | 1^+ \rangle}{\langle 0^- | O(E1) | 1^+ \rangle} \right)$$

$$3/2^+ \rightarrow 1/2^- \rightarrow 3/2^+ \qquad {}^{21}\mathrm{Ne}$$

$$A_{RL} = \frac{-2}{\Delta E}\left\langle \frac{1}{2}^+ \middle| H_{PNC} \middle| \frac{1}{2}^- \right\rangle \left(\frac{\langle 1/2^+ | O(M1) | 3/2^+ \rangle}{\langle 1/2^- | O(E1) | 3/2^- \rangle} \right) \left(1 + \frac{1}{4}\cos\theta\right)$$

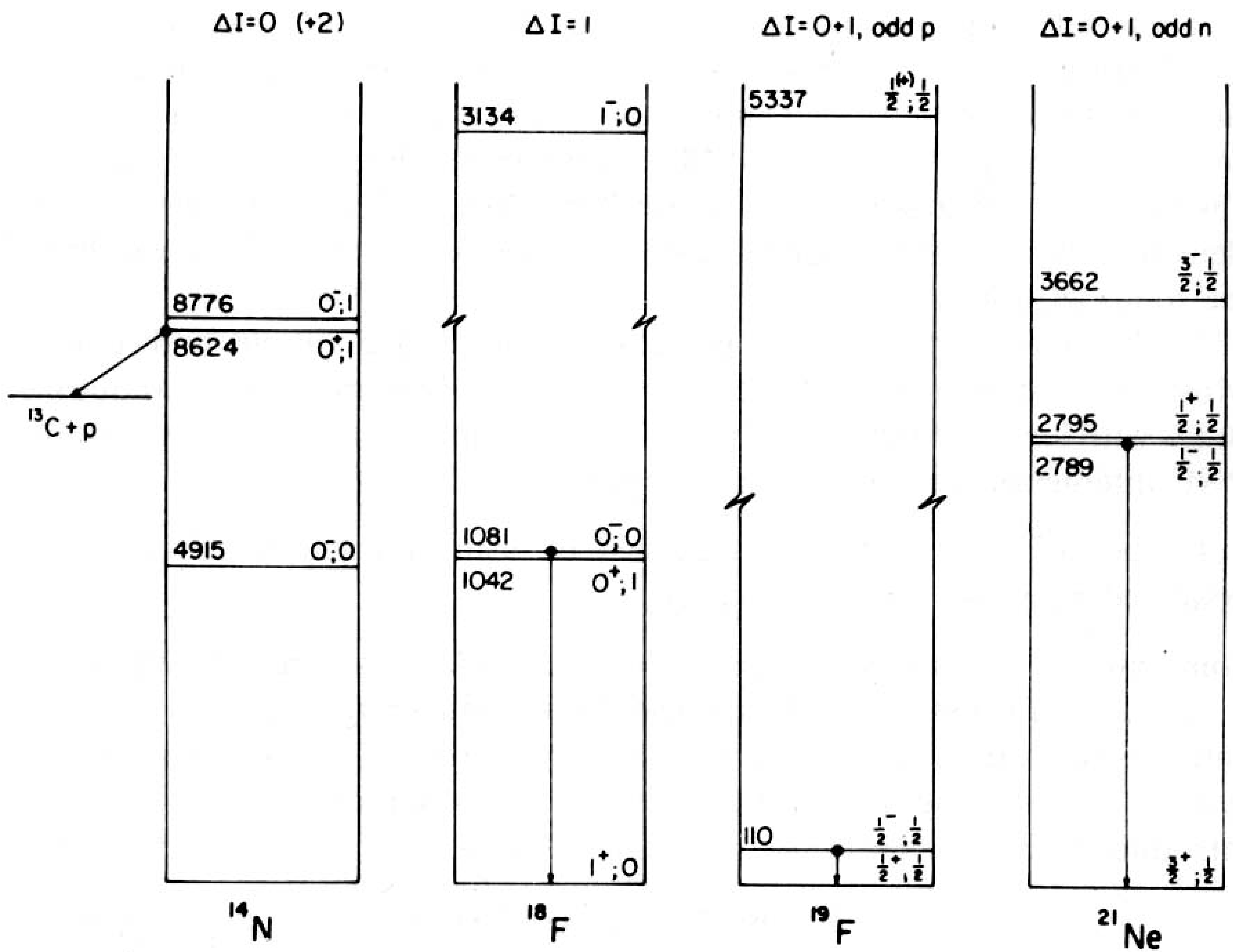

ΔE	152–206i keV	39 keV	110 keV	5.7 keV
$\Delta E'$	3703 keV	3134 keV	5337 keV	3662 keV
	$\sqrt{\Gamma_{0^-}/\Gamma_{0^+}} = 10.5$	$\lvert M1/E1 \rvert = 112$	$M1/E1 = 11$	$\lvert M1/E1 \rvert = 296$

Previous best result on ^{19}F

$$A_\gamma = -(7.4 \pm 1.9)\times 10^{-5}$$

30% error

Improvement is needed

Results of 2 hour measurement in March 2004

$$\frac{\Delta A_\gamma}{A_\gamma} = \frac{1}{1.4 A_\gamma}\sqrt{\frac{1}{N}}$$

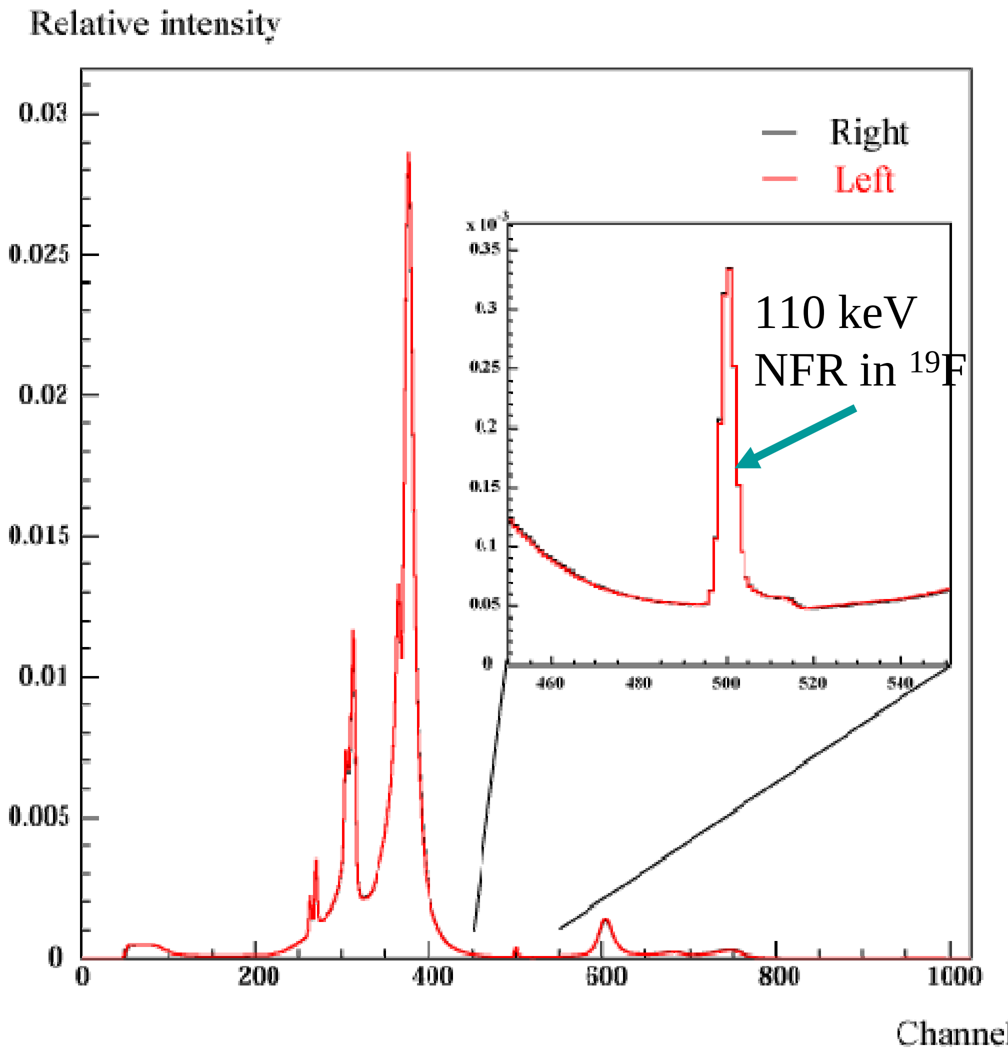

Scattered photon spectra. Black line is right-handed circularly polarized photon beam and red is left-handed. Each spectrum is normalized by total counts. The peak at 500 channel is Nuclear Resonance Fluorescence.

10% error measurement by independent method

Kawase et al.,

Experiment

Statistical error of asymmetry measurement

$$\frac{\Delta A_\gamma}{A_\gamma} = \frac{1}{\sqrt{2}A_\gamma}\sqrt{\frac{1}{N}}$$

$$A_\gamma \sim 10^{-4}$$

If we aim to get <15% error, we need to count over 10^9.

We have to do high counting rate experiment.

Teflon target : 100 μm $(CF)_2$

Photon intensity (110 keV : Circular polarization)

$I_\gamma \sim 10^{11}$ Photons/s/eV

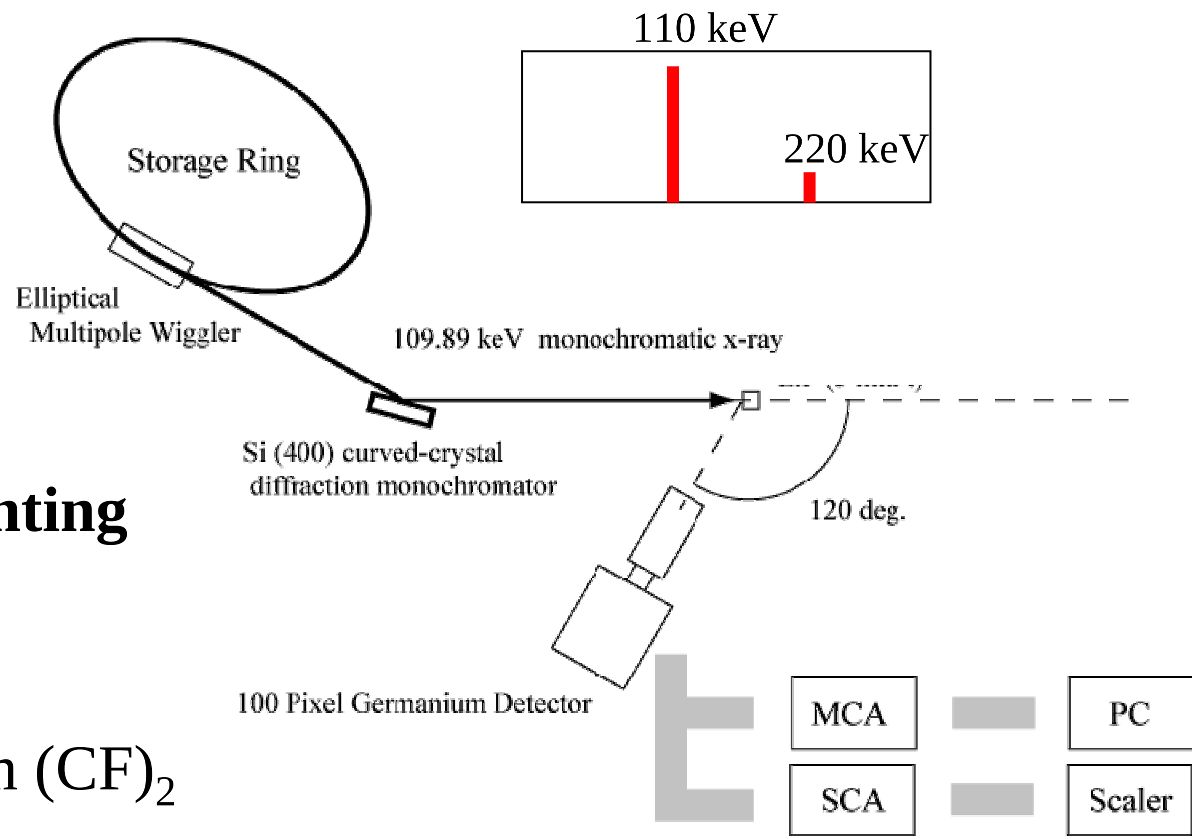

April 2005

110 keV ½+→1/2- transition in ^{19}F

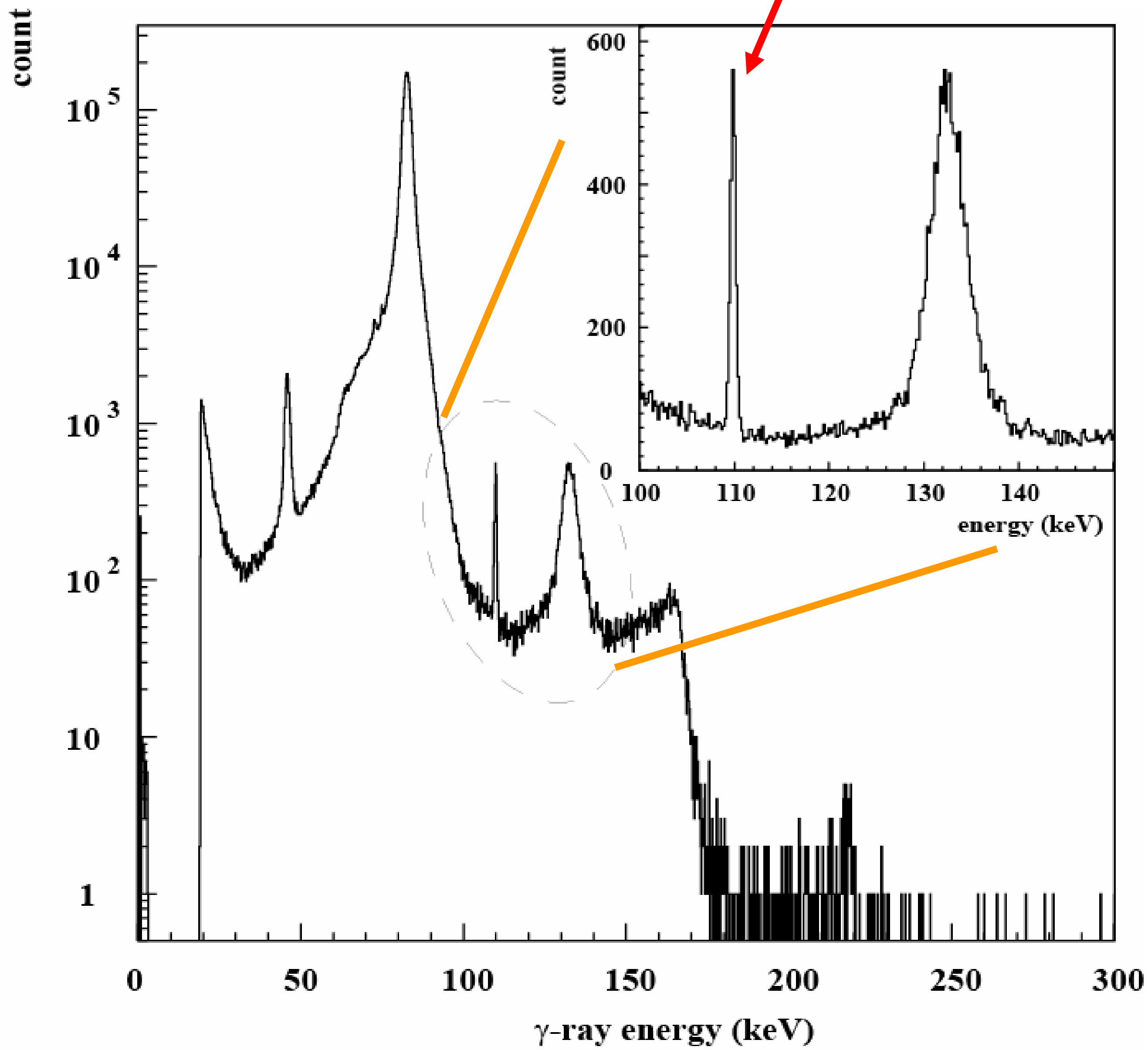

New scintillation crystal YSO (Y_2SiO_5:Ce)

^{241}Am 60 keV

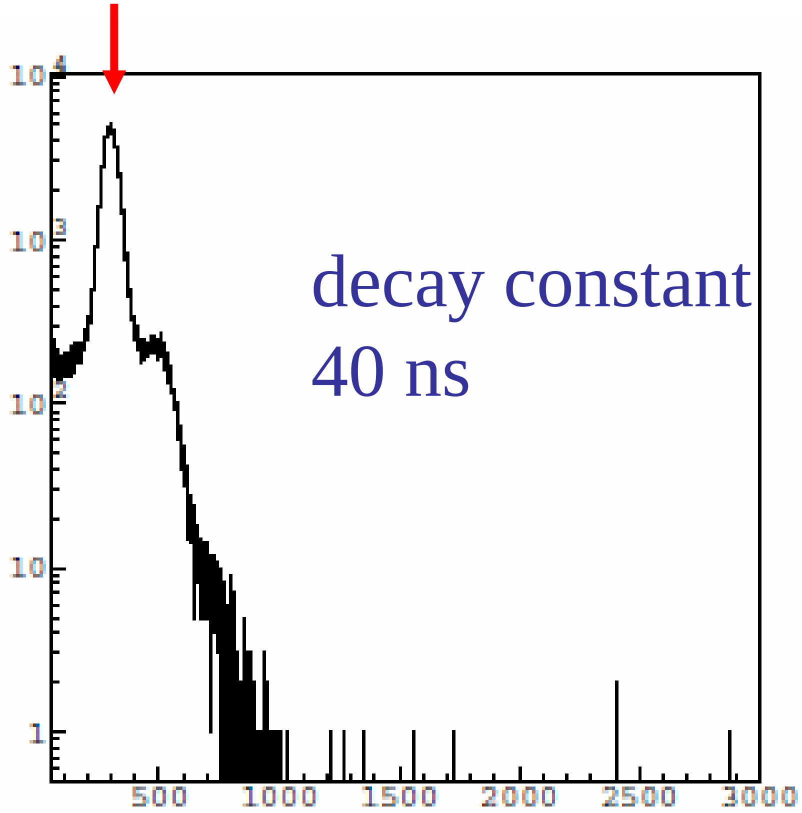

decay constant
40 ns

^{57}Co 122 keV

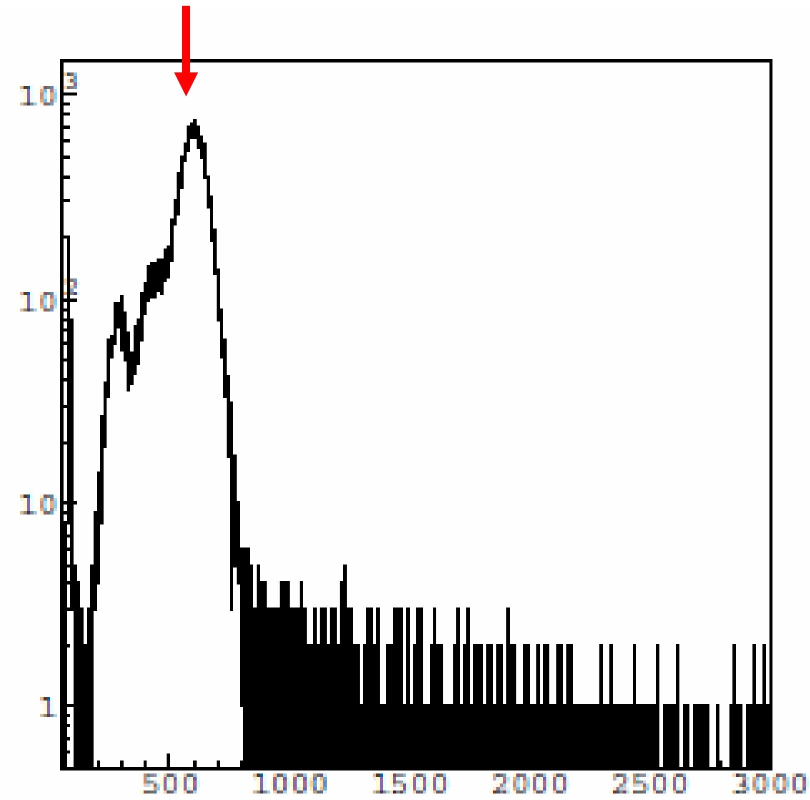

Table 1: comparision of resolution for scintilators (%)

	LYSO	~~YSO(no.1)~~	YSO(no.2)	GSO	NaI
59.54keV of ^{241}Am	10.44	~~10.45~~	10.58	16.41	10.94
122.06keV of ^{57}Co	9.87	~~8.85~~	8.87	10.70	11.75

Application to ferromagnetism

para-positronium annihilation

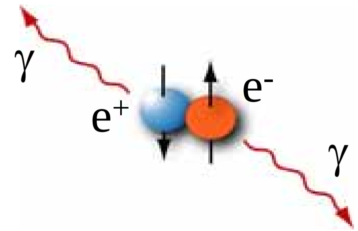

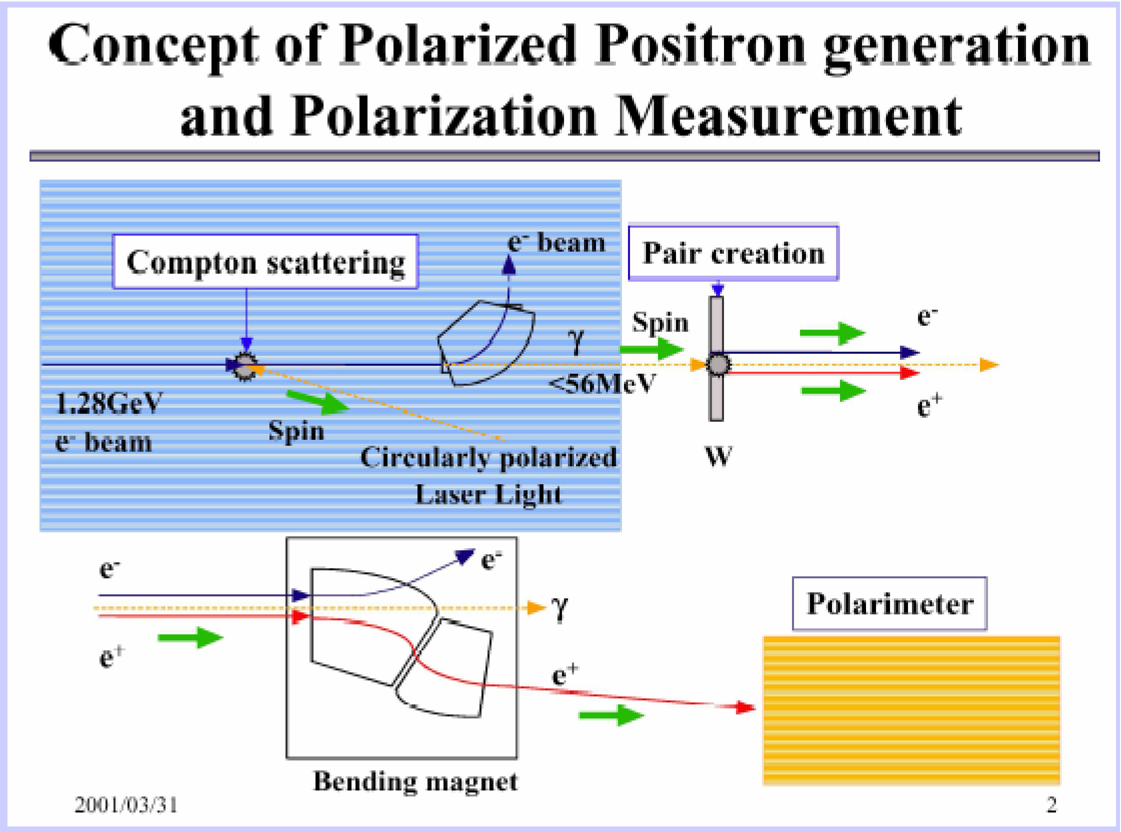

Experimental setup at ATF in Japan

Positron Polarization Demonstrated by Annihilation in Magnetized Iron*

S. S. Hanna and R. S. Preston

Argonne National Laboratory, Lemont, Illinois

(Received April 29, 1957)

PR 106, 1363 (1957)

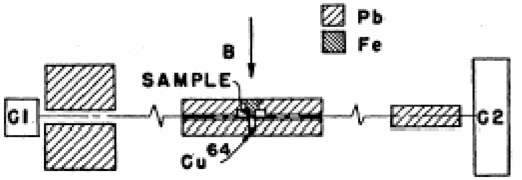

Fig. 1. Experimental arrangement.

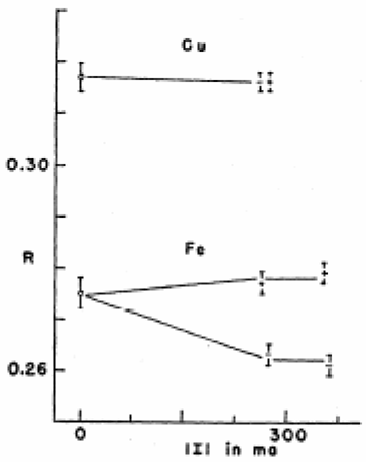

Fig. 2. Normalized coincidence rate R, as defined in the text, plotted against the magnet current. For the (+) points the magnetic field was parallel to the direction of motion of positrons. For the (−) points the field was reversed. The lines are supplied merely to aid in visualizing the data. Fe and Cu signify annihilation in the iron sample and copper sample, respectively.

ultra high intensity laser

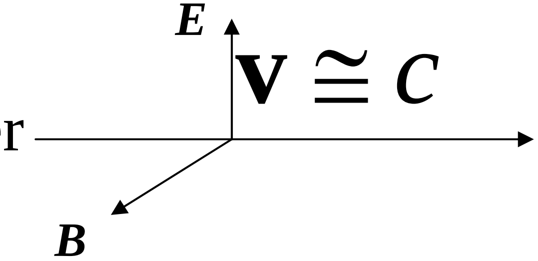

$$\mathbf{F} = e\mathbf{v} \times \mathbf{B}$$

Laser Acceleration

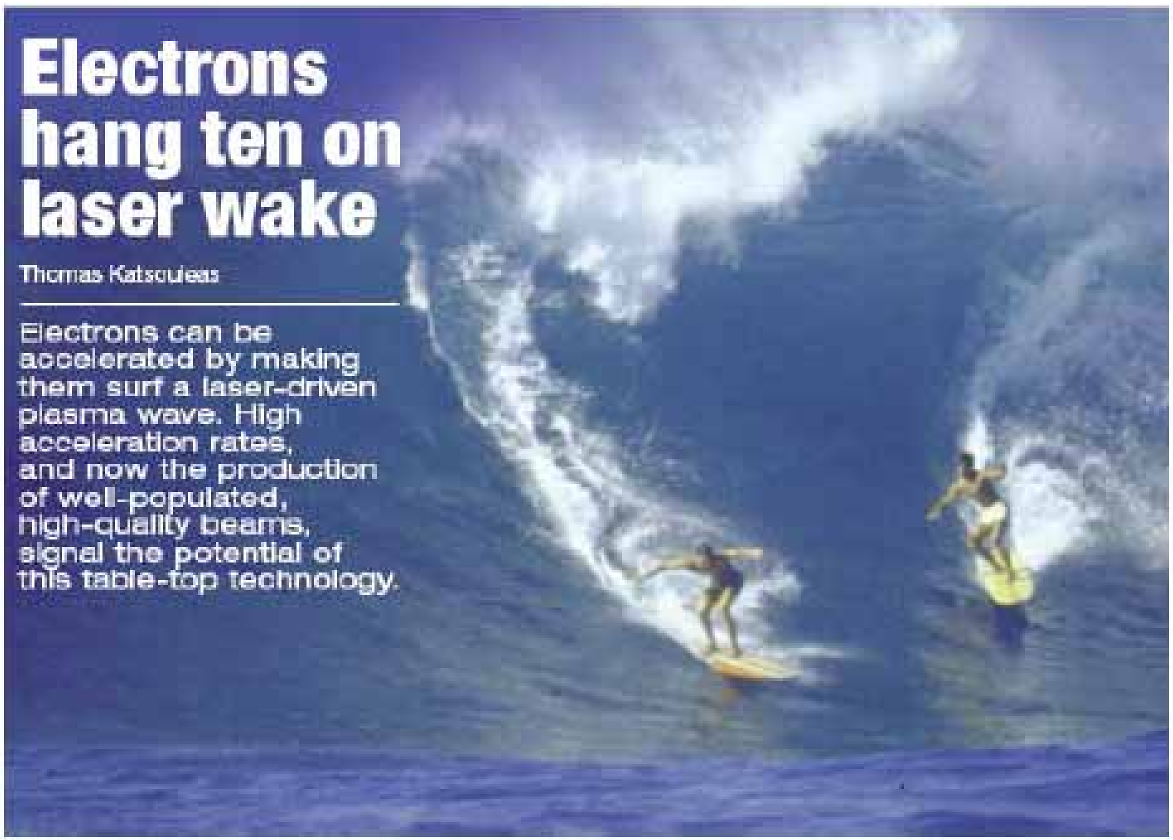

Electrons hang ten on laser wake

Thomas Katsouleas

Electrons can be accelerated by making them surf a laser-driven plasma wave. High acceleration rates, and now the production of well-populated, high-quality beams, signal the potential of this table-top technology.

Nature 431 (2004) 535 UK
431 (2004) 538 US
431 (2004) 541 France

Mono energetic electron beams from Laser Wakefield Accelerator

Mono energetic high quality electron beams first produced by AIST(JAPAN), IC/RAL(UK), LOA(FRANCE), LBNL(US), and JAERI-CRIEPI(JAPAN)

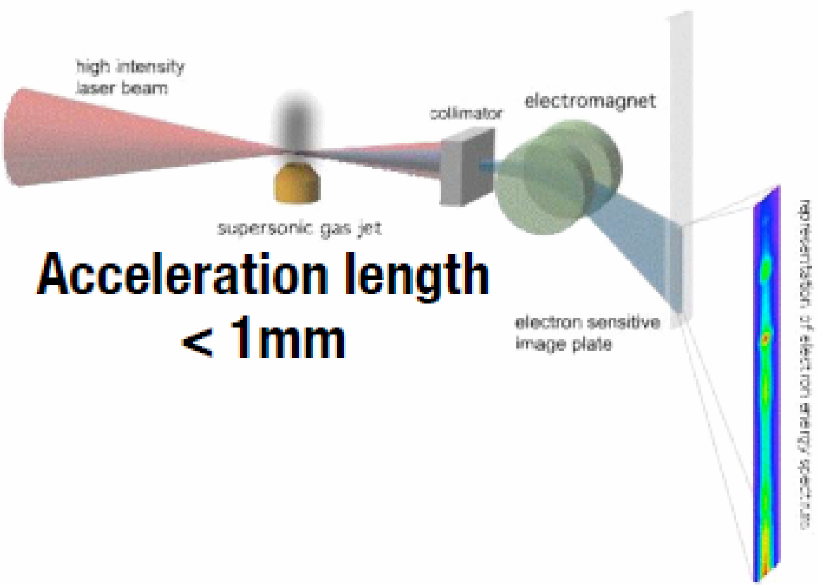

Acceleration length < 1mm

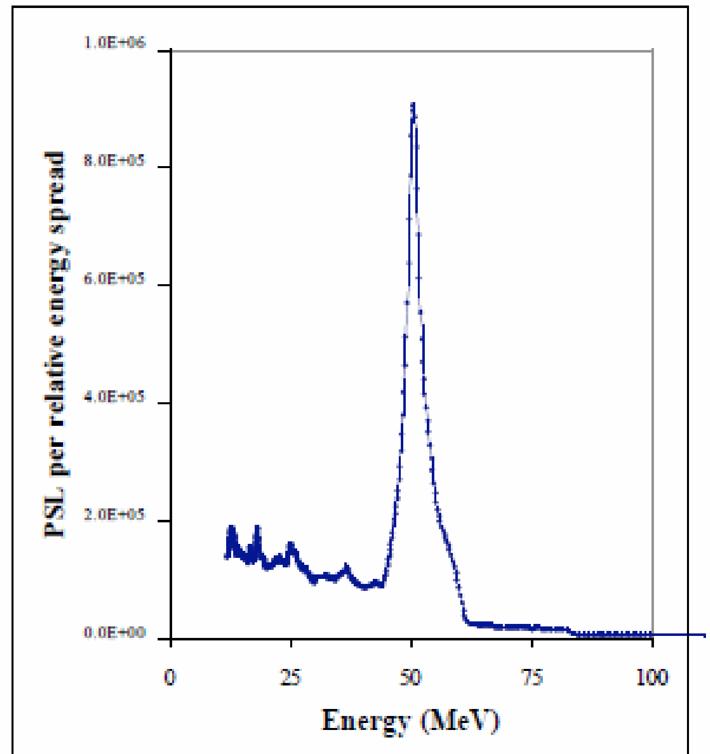

C. Murphy et al., IC/RAL, UK

Nature 431 (2004) 535

The LCLS
(Linac Coherent Light Source)

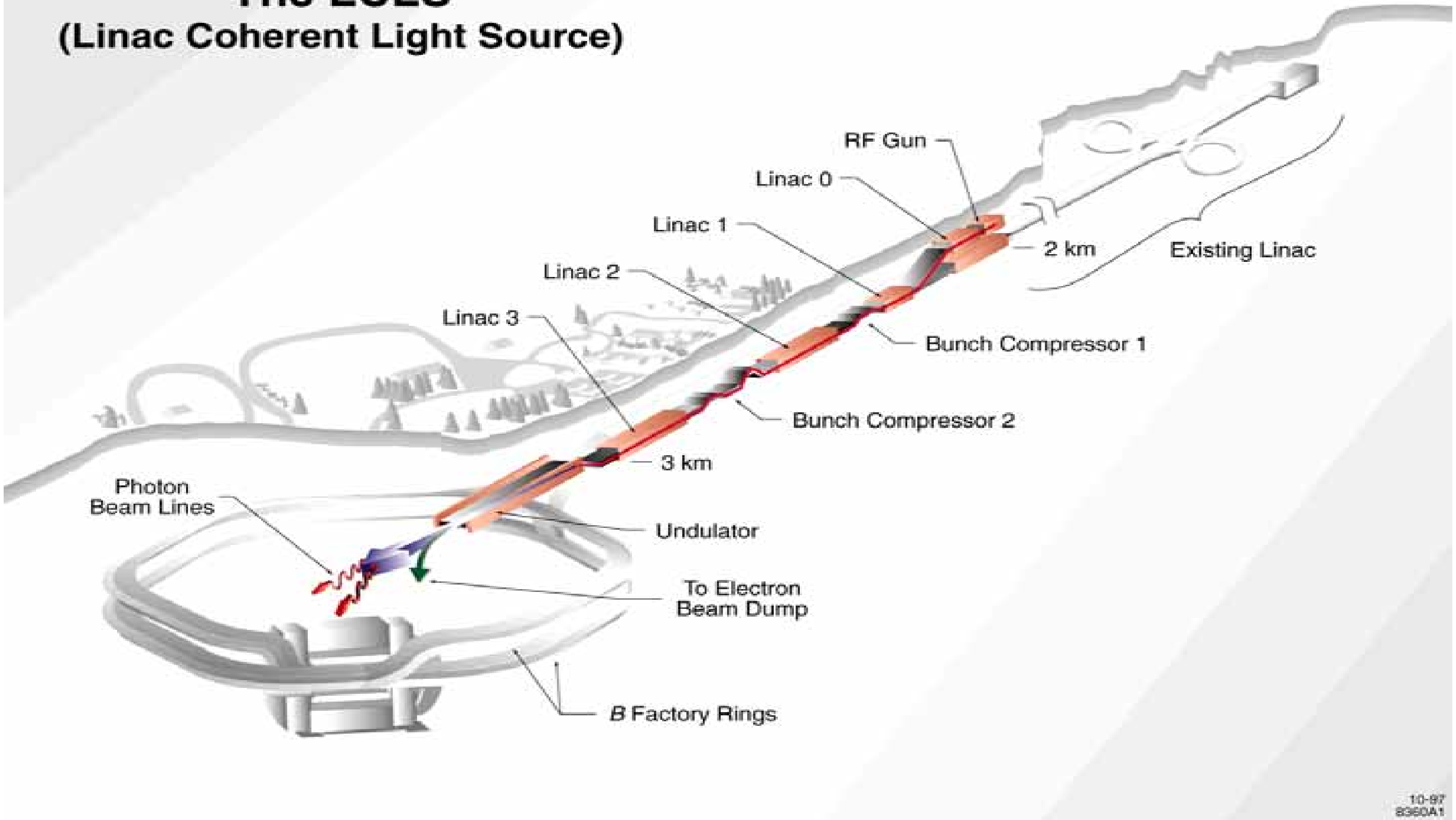

Performance Characteristics of the LCLS

Peak and time averaged brightness of the LCLS and other facilities operating or under construction

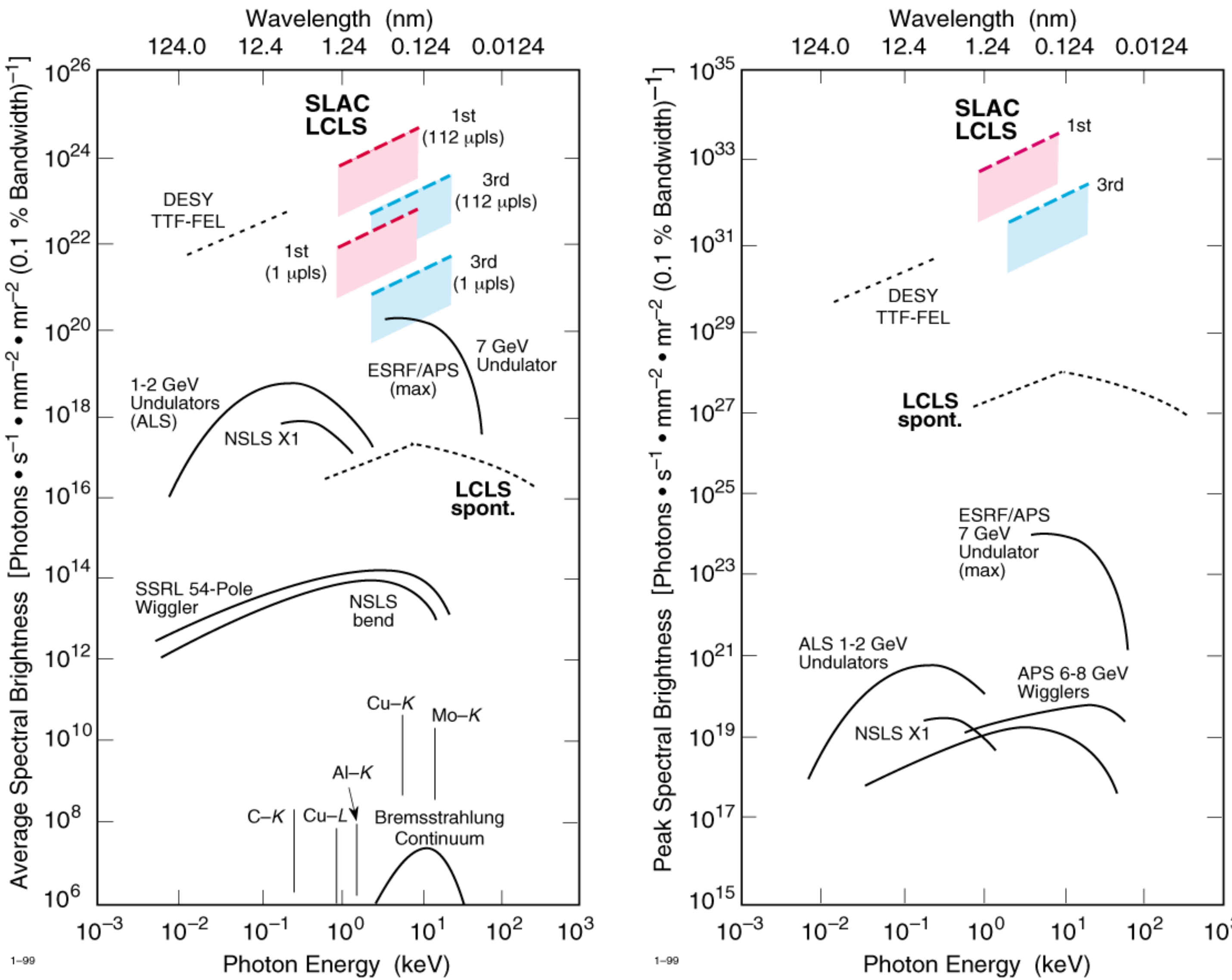

まとめ

光ビームの強度は今後指数関数的に伸びる。

X線FELなど将来のノーベル賞に結びつくような革新的技術の発展。

光科学、光核科学の推進。

チャレンジ、チャレンジ、新しいアイデア